ULTRASONIC VELOCITY MEASUREMENTS OF PRECAMBRIAN METAMORPHIC ROCKS AND THEIR CORRELATION WITH FIELD MEASUREMENTS

Thesis for the Degree of M. S.

MICHIGAN STATE UNIVERSITY

James T. Whitaker

1966

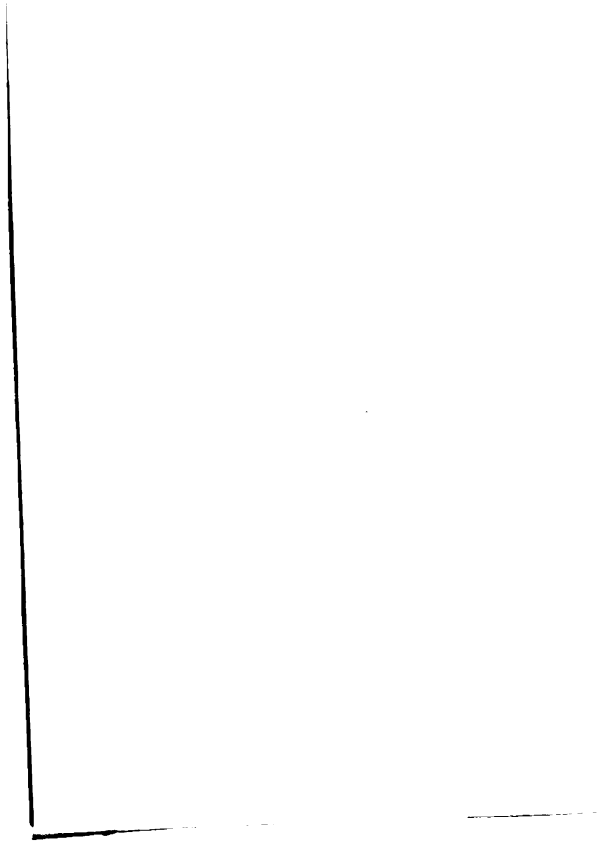

ABSTRACT

ULTRASONIC VELOCITY MEASUREMENTS OF PRECAMBRIAN METAMORPHIC ROCKS AND THEIR CORRELATION WITH FIELD MEASUREMENTS

by James T. Whitaker

A comparison between compressional wave velocities measured by standard seismic methods on outcrops of Precambrian metamorphic rocks and laboratory velocity measurements on specimens collected from the same outcrops reveals that the field velocities are much lower and exhibit larger anisotropies. The only significant geological difference between the two sets of measurements is the greater degree of fracturing in the outcrop, to which is attributed the difference of velocities and anisotropies. Fractured laboratory specimens are found to have a lower velocity and a higher anisotropy than non-fractured specimens of the same lithology, which substantiates the previous conclusion. The laboratory velocities on the non-fractured specimens reveal that the basic igneous rocks are the most isotropic, and that the gneisses and schists are the most anisotropic.

In addition to the compressional velocities, shear wave velocities were measured for 21 of the laboratory specimens. The five elastic constants were calculated

from the two velocities and the density. The rate of increase of compressional wave velocity with density for these 21 specimens is 3.07 km/sec per g/cc which is in very good agreement with the value of 3.05 km/sec per g/cc found by Birch (1961). The shear velocity has a rate of increase of 0.94 km/sec per g/cc. The elastic constants increase with density at the following rates: Lame's constant, 77 x 10^{10} dynes/cm^2 per g/cc; shear modulus, 29 x 10^{10} dynes/cm^2 per g/cc; Poisson's ratio, 0.21 per g/cc; bulk modulus, 94 x 10^{10} dynes/cm^2 per g/cc; and Young's modulus, 84 x 10 dynes/cm per g/cc. Densities of the 73 laboratory specimens range from 2.62 to 3.67 g/cc.

The laboratory velocity measurements employed transducers with a fundamental frequency of 360 kcps for the compressional waves and 260 kcps for the shear waves. The accuracy is 2% for the compressional wave velocities, and 3% for the shear wave velocities.

ULTRASONIC VELOCITY MEASUREMENTS OF PRECAMBRIAN METAMORPHIC ROCKS AND THEIR CORRELATION WITH FIELD MEASUREMENTS

By

James T. Whitaker

A THESIS

Submitted to
Michigan State University
in partial fulfillment of the requirements
for the degree of

MASTER OF SCIENCE

Department of Geology

1966

ACKNOWLEDGMENTS

The author wishes to express his appreciation to:

Mr. Charles Washburn for his aid in identifying and in sampling outcrops in the Espanola, Ontario area.

The Bendix Systems Division, Ann Arbor, Michigan for allowing the author to use their calibrated electronic equipment for the velocity measurements. Mr. Walter Dobar and Mr. Herbert Tobey are especially thanked for their instruction concerning the operation of the equipment and for much assistance in solving problems encountered during the measurements.

Dr. James Trow and Dr. Justin Zinn of the Geology Department, Michigan State University, for their helpful suggestions and criticisms of the manuscript,

Dr. William Hinze, Geology Department, Michigan State University, to whom sincere gratitude is expressed for helpful guidance, advice, and criticism to the author throughout this study.

TABLE OF CONTENTS

LIST OF TABLES

LIST OF FIGURES

CHAPTER I

INTRODUCTION

The recent development of the ultrasonic pulse technique makes it possible to determine the characteristic velocity of laboratory specimens of rocks. This technique has been used to investigate the factors controlling velocity and to study variations of elastic constants among rocks. The principal objective of the present work is to examine the effect fractures have on velocity by comparing measurements on rocks with many fractures to measurements on the same rocks with relatively few fractures. The former measurements were made on lamellar outcrops over distances of 25 to 80 feet, and the latter were made on specimens collected from these outcrops and cut into cubes containing as few fractures as possible. The secondary objective is to determine the five elastic constants for the laboratory specimens, and to examine their variation with density.

To accomplish these objectives, samples collected mainly from the areas of Marquette, Michigan and Espanola, Ontario were cut into 73 cubes, representing 34 metasedimentary and meta-igneous lithologies and one sedimentary

lithology. Sixteen of these cubes are from the outcrops of the field velocity study. The density of the cubes was determined by the weight-loss-in-water method. The compressional and shear wave velocities were ultrasonically determined between the three pairs of opposite faces of the cubes. From these measurements the following were calculated for each cube: the compressional wave anisotropy, the average compressional and shear wave velocities, and the five elastic constants. It is these quantities that are studied in this paper. Velocity anisotropy is defined as a variation of velocity with direction. In this study, anisotropy is represented as the average of the two highest velocities minus the minimum velocity, divided by the average of all three velocities, and multiplied by 100; $\frac{V_{max_{ave}} - V_{min}}{V_{ave}} \times 100$.

The field measurements on compressional wave velocity anisotropy were made by Merritt (1961) on seven vertically dipping lithologies in the Northern Peninsula of Michigan by conventional seismic methods. The geophone spread lengths ranged from 25 to 80 feet and were oriented perpendicular and parallel to the structural orientation of the outcrop. Samples for the laboratory study were collected from all five of his outcrops and from an outcrop close to one of his areas (Siamo slate) covered by unconsolidated sediments. The cubes for the laboratory study were cut

from the collected samples so that one pair of faces is parallel to, and two pairs of faces are perpendicular to, the structural orientation of the rock. It was anticipated that, if fractures lower velocity, the velocity isotropism would be higher in the cubes than on the outcrops. The fractures in the outcrop are predominately parallel to the structure, which will cause the velocity to be reduced greater in a direction perpendicular to the structure than parallel to it. This isotropism should be lower than that in cubes of the same material because the latter have no, or very few, fractures. The outcrops also have a few fractures intersecting the structural orientation which will lower the velocity measured in all directions. The cubes have fewer fractures and therefore their velocities would be expected to be higher.

From the density and the compressional and shear velocities, Lame's constant (λ) shear modulus (μ), Poisson's ratio (σ), bulk modulus (K), and Young's modulus (E) are calculated and correlated with density. All five constants were expected to increase with density at rates which were unknown because of limited studies pertaining to the problem.

Previous Investigations

Laboratory velocity determinations on rock specimens were first made by Zisman (1933), but ultrasonic determinations of velocity could not be made until technology

developed during World War II improved the necessary electronic equipment. Hughes, working with Jones and Cross (1950, 1951) pioneered in the application of the ultrasonic pulse technique to velocity determinations in geology. Wyllie, Gregory, and Gardner (1956, 1958) studied the effects of porosity and fluid content on velocity. Peselnick and Outerbridge (1961) found that shear velocity is independent of frequency from 4 to 10,000,000 cycles per second (cps). It is commonly assumed that compressional velocity also is independent of frequency, but no thorough study of frequency dispersion has been conducted. Birch (1961) compared laboratory compressional velocities, in the 1 Mcps range, for three granites with previous field velocity studies (roughly 100 cps). He found his velocities at about 10 bars (10 atmospheres) pressure corresponded to the field velocity determinations made over distances of 1700, 3000, and 4600 feet. This is given as evidence for the lack of frequency dispersion of velocity, for if velocity varied significantly with frequency, the velocities of these two methods would not agree.

Birch (1960, 1961) has thoroughly studied the effects of pressure, up to 10 kilobars, on compressional wave velocity, and Simmons (1964) has duplicated the work for shear velocity but has not published an analysis of his data. They found that both velocities increase with pressure. The largest effect is at low pressure and is

attributed to fractures closing and providing a faster path for the elastic wave. The smaller pressure effect at higher pressures is an intrinsic property of the material. Birch suggests a pressure of at least 500 bars is necessary to eliminate the effect of fractures.

Tocher (1957) studied the ultrasonic compressional wave velocity anisotropy induced by the simple axial compression of five rocks. His measurements were made perpendicular and parallel to the applied stress. The closing of fractures perpendicular to the stress, increasing velocity in only that direction, is probably the cause of the anisotropy he measured.

No detailed study has been made comparing field and laboratory velocities of the same rocks. Birch (1961) found that laboratory and field measurements did agree for three granites in a superficial treatment of the problem.

Zisman (1933) compared statically determined elastic constants with constants derived from field determined velocities and found generally poor agreement, which he attributed to pores and fractures in the outcrops of the field work. Hughes and Jones (1950) studied the variation of elastic constants with temperature and pressure in five igneous rocks and found that they increase with pressure and decrease with temperature, except for Poisson's ratio which had small and erratic changes. Peselnick (1962) found that the constants increased with density and

decreased with saturation for the Solenhofen limestone at atmospheric pressure.

Woeber, Katz, and Ahrens (1963) calculated from ultrasonically measured velocities the elastic constants of 32 rocks and 13 minerals, and have been the only workers to use rock cubes rather than cylinderical cores. Only by measuring elastic properties in different directions in the same specimen can anisotropy be truely determined, and this can be done only in cubes. The section of the present work on elastic constants is patterned after their work, using cubes two inches on a side rather than one inch to obtain more typical velocities. In all previous works homogeneous rocks were studied, but in this study most specimens were especially selected for their non-homogeniety.

CHAPTER II

DESCRIPTION OF SPECIMENS

Introduction

A comparison of velocity anisotropy measured in the laboratory with field measurements is a major part of this study, and therefore the sites of previous field measurements were included as sites for collecting laboratory specimens (Figure 1). Other rocks from the Northern Peninsula of Michigan also were included in this study to increase the variety of lithologies and to extend the range of density and velocities of the specimens. Samples also were collected from the Espanola, Ontario area, on the north shore of Lake Huron because this area was known to have many outcrops and fresh road cuts in metasedimentary rocks. The author was aided in the Marquette, Michigan area by Dr. Justin Zinn, Geology Department, Michigan State University, and in the Espanola, Ontario area by Mr. Charles Washburn, Senior Assistant of the Ontario Department of Mines party mapping the area, headed by Mr. Ken Card.

The Grenville granite gneiss was collected by Dr. Harold Stonehouse, Geology Department, Michigan State University, from the area of Parry Sound, Ontario and is included

because its anisotropy was expected to be very large due to its pronounced gneissic texture. The Quincy granite (from Massachusetts) was obtained from the Michigan State University, Geology Department rock samples for the purpose of comparing velocities found in this study with those previously reported for this lithology. The Littleton granite gneiss was collected by David Chipman from Crawford Notch, New Hampshire and is included to increase the number of specimens of granite gneiss.

Lithologies Collected from the Northern Peninsula of Michigan

The outcrops studied by Merritt (1961) in the Northern Peninsula of Michigan (Figure 2) were selected by him because they were "lamellar either in the form of banding, fracturing, bedding, or mineral orientation." Cubes 1, 2, and 3 are from his Area "A," an outcrop of Goodrich quartzite and Negaunee iron formation located in the SW 1/4, sec. 6 [not 16], T. 46 N., R. 29 W., Marquette County, near the town of Republic. This outcrop was difficult to find and the Negaunee iron formation collected from this location may not be from the identical outcrop of the field study. The outcrop chosen as a collection site is immediately east of an abandoned mining trench and is 100 yards northwest of where County Road 601 joins with the road running west from Republic to M95. The pronounced banding strikes N45°W and dips vertically

with no contortion. The alternating bands are of magnetite and recrystallized chert, and vary in width from 0.05 to 0.5 inches in the three cubes cut from samples of this outcrop. The volume percentage of magnetite in the cubes based on visual inspection varies from 20 in cube 2 to 50 in cube 1. While small areas of the outcrop may have a composition outside this range, it is very unlikely that the average of the area covered by the 60 foot seismic spread could have a composition outside of this range. The Goodrich quartzite was not found on this outcrop and none was collected for this study.

Cubes 4, 5, and 76 were collected from area "B" of the field study at the south end of the new M95 bridge over the Michigamme River, just west of Republic in the SE 1/4, sec. 1, T. 46 N., R. 30 W., Marquette County. The lithology is a former diabasic dike metamorphosed into a "vertically banded garnetiferous biotite amphibolite schist" which has been "highly contorted" and whose "stratigraphic position is either upper Goodrich, Michigamme, or Greenwood" (Merritt, 1961). The laboratory specimens show a slight schistocity but no contortion.

Cubes 6 and 7 were collected from Lighthouse Point which is Merritt's field area "C" at 46° 33' longitude and 87° 23' latitude. The Mona schist is well exposed here, and the foliation strikes east-west and dips 65° N. There are many large fractures striking north-south and dipping 85° E.

Another set of fractures striking north-south and dipping 20° also is present. The outcrop is a hard greenstone of pronounced schistocity, composed of "epidote, chlorite, hornblende, plagioclase, and quartz" (Van Hise and Leith, 1911).

Cubes 8 and 9 are from area "D" on the northeast shore of Presque Isle, Marquette City (46° 35' longitude, 87° 23' latitude) where a large area of serpentinite altered from periodotite is exposed. The linear pattern of the outcrop is due to weathering or alteration along fractures with no visible grain orientation or banding. The fractures strike N 30° W and dip vertically, and are spaced from 0.25 inches to 3 feet apart. No other fractures were noticed at the outcrop, but cube 8 has three mutually perpendicular fractures in it.

Cubes 10 and 11 were collected at Merritt's area "E," south of the main field study area in the NW 1/4, sec. 10, T. 41 N., R. 30 W. Dickinson County, Michigan, where much granite gneiss is exposed. The samples collected are from an outcrop near the convergence of the road and railroad. The gneissic foliation strikes N 50° W and has a vertical dip. The outcrop is lichen covered and, the rock's color is made lighter to a depth of 0.5 inches by weathering. The gneissic texture appears much weaker in the cubes than on the outcrops.

No samples were collected from Merritt's area "F." This area has 55 feet of unconsolidated sediments overlying horizontal beds of Negaunee iron formation. The anisotropy measured in the field therefore was in two directions parallel to the banding, and no velocity was measured perpendicular to the beds. Because the area is drift covered and the real anisotropy was not measured, no samples were collected from this area.

Specimens 12 and 13 of the present study were collected about 4 miles west of area "F," on Jasper Knob, Ishpeming. This is a highly contorted outcrop of Negaunee iron formation. The laboratory specimens from this location are composed of hematite and chert (no magnetite as in cubes 1, 2, and 3) in alternating bands less than 0.1 inches wide, with a small amount of contortion. While no open fractures can be seen in the cubes, there are many hairline cracks in cube 13 and the rock tends to split along the bands while cutting in that direction.

Merritt's area "G" is in the N 1/2 of NE 1/4, sec. 8, T. 47 N., R. 26 W., Marquette County and is covered by unconsolidated sediments. The bedrock is Siamo slate dipping 40° SW. Cubes 14 and 15 were collected just north of this area, 0.5 miles east of the Jones and Laughlin Ore Research Lab, where the road is cut into the slate. Here the slate is dark, brittle, and easily split along the cleavage which strikes N 75° W and dips 80° S. It was very

difficult to find samples which were not split along the cleavage, and to cut parallel to the cleavage without splitting the specimen. Each of the test cubes has one visible parting along the cleavage.

This concludes the discussion of the samples collected from Merritt's field study areas. Other lithologies were collected in the same general area and their description follows.

Cubes 16, 17, 18, 19, 20, and 21 were collected from Chocolay Quarry in the NE 1/4, sec. 1, T. 47 N., R. 25 W., Marquette County. At the south end of the quarry the Mona schist of Keewatin age is exposed. The cleavage is pronounced and makes it difficult to obtain a competent specimen 2 inches thick. The Mona schist here differs from the Mona schist of Lighthouse Point in that it is much softer, more fissile, and has a contorted schistose structure. At Lighthouse Point the foliation is straight and very pronounced, and the outcrop is cut by two other sets of fractures. Mona schist specimens from Chocolay Quarry (cubes 16 and 17) show bands about 0.1 inches thick with small pebbles of quartz and much chlorite and mica.

Cubes 18 and 19 were cut from Mesnard quartzite, which is near the base of the Huronian (Animikie) Series and is exposed over most of the quarry face. It has a vitreous luster and a white to dark gray color. The strike is N 65° W and the dip is 35° E. Faint bedding can be seen

in the test cubes which contain many healed fractures. The rock is about 99% quartz with a small amount of iron oxide in the healed fractures (Van Hise and Leith, 1911).

About 200 yards northwest of the Quarry cubes 20 and 21 were collected from a cliff of Kona dolomite. It is stratigraphically above the Mesnard quartzite and contains algal structures which indicate the formation is horizontal at this point. There are a few healed fractures in the dark pink test cubes.

On U. S. Highway 41 at a road cut 3.4 miles west of the Washington Street junction in the NW 1/4, sec. 24, T. 48 N., R. 26 W., Marquette County is an outcrop of dark gray basalt with pillow structures. Only one sample was collected, and the cube cut from it, cube 22, shows five parallel fractures in it.

A sample of quartz latite porphyry, cube 23, was collected from the northeast side of Lighthouse Point. The exposure is very small and shows pronounced jointing at right angles. The laboratory specimen shows elongated grains of quartz (up to 0.2 inches long) and many round ones 0.1 inches in diameter. Roughly parallel to the elongation of the grains are a few nebulous lines which probably are healed fractures.

An amphibole biotite schist, cubes 24 and 25, was collected from a dike in Townsend Ely Roadside Park near the west end of Lake Michigamme (SW 1/4, sec. 20, T. 48 N.,

R. 30 W., Marquette County). US41 cuts through this rock formation which strikes N 40° W. and dips vertically. The cube faces show laths of amphibole in a ground mass which was identified as an aggregate of biotite by thin section analysis. The laths can be found in any orientation, but they rarely cut across the lineation of the specimen. Cube 25 has several grains of pyrite on one face.

Cubes 26 and 27 were cut from Republic granite which was collected at a road cut about 4 miles north of Republic and 100 yards north of the Chicago, Milwaukee, St. Paul, and Pacific Railroad crossing of M 95 (SW 1/4, sec. 20, T. 47 N., R. 29 W., Marquette County). The specimens have numerous small fractures of random orientation. The majority of the granite is feldspar (crystals up to 1 inch long) embedded in quartz with a small amount of biotite.

Lithologies Collected From the Espanola, Ontario Area

The second principal collection area is 175 miles east of Sault St. Marie, Ontario and extends south from Espanola, Ontario along Highway 68 thirty miles to the tip of Cloche peninsula (Figure 3). The Bruce and Cobalt Series of the Huronian Period are exposed in numerous outcrops with many fresh road cuts in the metasedimentary formations. Samples were collected from the oldest formation, McKim graywacke, up through the youngest, the Lorrain Quartzite, and include later igneous intrusions, most of which have been metamorphosed.

The McKim graywacke, cubes 31 and 32, was collected at the north end of the new highway bridge over the Spanish River at Espanola. This is the oldest formation sampled, but its geologic age is in question. It may be the upper formation of the Sudbury Series or the lowest formation of the Bruce Series, below the Mississagi quartzite. The samples of McKim were collected from a large road cut which revealed gentle folds plunging N 70° E at a 25° dip. Thin section examination shows it to be a micaceous quartzite composed of more than 70% fine quartz with some biotite and chlorite.

The Mississagi quartzite (cubes 33 and 34) is normally considered as the base of the Bruce Series. Samples of it were collected from the Duplessie farm one mile east of Espanola. Cube 33 has cross-bedding with beds up to 0.6 inches thick, and cube 34 has thin, parallel beds. Quartz is the only significant mineral, and the grains are up to one millimeter in diameter. Cube 33 has a fracture which may not be completely healed. It diagonally cuts the cube so that an energy pulse traveling between any pair of faces would have to cross it.

Cubes 35, 36, 37, and 38 are Espanola limestone which was collected from two locations and may be either the Bruce or Espanola limestone of Quirke (1917). The Ontario Department of Mines has found in its recent mapping that the distinctions used by Quirke are not always valid, and that

it is difficult, if not impossible, to tell the Bruce from the Espanola limestone. If Quirke's distinction of formation thickness is correct (150 feet for Bruce and 25 feet for Espanola), then the formation sampled is the Bruce because it is at least 100 feet thick at both locations.

At both collection sites the beds are vertical, striking about 90° E. The first site is about 0.5 miles west of Highway 68 where the railroad tracks cross the east end of Haystack Harbor, Bay of Islands. The other site can be reached only by boat and is on Island T.P. 2203 in the west channel around Iroquois Island, McGregor Bay. At both locations the layers with the highest quartz content stand out and make the surface very rough. It was possible to collect only from these quartz-rich ridges so that the laboratory specimens contain more quartz than is typical for the formation. A thin section shows about half calcite, and a large proportion of quartz and biotite with some chlorite. The cubes from Haystack Harbor (cubes 35 and 36) do not show the bedding as well as cubes 37 and 38 from Island T.P. 2203. In cube 38 the layers are uniformly about 0.1 inches thick, while in cube 37 they are lenticular up to 0.2 inches thick.

The Espanola argillite (cubes 39, 40, 41, and 42) was collected from the shore of Clear Lake (formerly Griffin Lake) near Highway 68 and also from Pot Hole Portage at the west end of Iroquois Bay, McGregor Bay. Samples from

the first site show fine laminations, while those from the second site have bands of dark and medium gray color up to 0.7 inches thick. The latter outcrop is pale red, smooth, easily scratched and has prominent bands striking N 80° E and dipping 75° N. The small outcrop at Clear Lake has pronounced bands from 0.1 to 4 inches wide which strike N 80° W and dip 45° S. The carbonate content of this argillite outcrop was revealed by its effervescence when treated with 10% hydrochloric acid. A thin section of the Pot Hole Portage argillite shows a large amount of fine grained quartz with the remaining material being too fine grained to distinguish. Cubes 39 and 41 have fractures which probably would not effect the velocity measurements, but cube 42 has two partings along the laminations which would have to be crossed by an energy wave traveling perpendicular to them.

Cubes 43 and 44 were cut from the Serpent quartzite, collected at a new road cut near the east end of Raven Lake. This outcrop of the upper formation of the Bruce Series has limonite stains and bedding planes which strike east-west and dip 70° S. Grains about 0.5 mm. in diameter can be seen in both cubes, but bedding is seen only in cube 43.

The lowest formation of the Cobalt Series is the Gowganda which is of glacial origin. The formation has a variable composition including a banded argillite (cubes

45, 46, 47, 48 and 49) which was collected in two locations for this study. The first location is at a road cut through the nose of an anticline near the east end of Raven Lake. Here the beds strike N 35° E and dip 35° S, and the cleavage strikes N 65° E and dips 80° N. Cube 45 was cut from a sample which showed prominent banding, but no fracture pattern. Cubes 46 and 47 were cut from the same sample which displayed banding, and a fracture pattern cutting it at about 30°. Cube 46 was cut so that one pair of faces was parallel to the banding, and cube 47 was cut with one pair of faces parallel to the fracture pattern. The latter cube has one open fracture near the front face. The second collection site of Gowganda argillite was just east of the Whitefish Falls railroad station where the outcrop has conspicuous dark reddish-brown and black bands less than 0.2 inches thick. The strike of the bands is N 80° W, and the dip is 70° N. The bands in cube 48 are very vague, but are clearly seen in cube 49 which has a bad fracture parallel to them.

The Lorrain quartzite of the Cobalt Series is the youngest metasedimentary formation in the Espanola area and forms the dominant topographic feature of this area, the La Cloche Mountains. Recently it has been divided into gray, pink, green, white, and banded cherty units all of which were sampled, with the exception of the green unit. The gray Lorrain quartzite (cube 50) was collected at the

turnoff to the Jo-Ami Mine, about 100 feet south of where Highway 68 crosses a stream flowing into Charlton Lake. This is about 200 feet south of the Gowganda formation where the Lorrain has a strike of N 65° E, dipping 80° N. The cube has a weak banding with grain size uniformly less than 0.05 inches and has no visible fractures. The pink Lorrain quartzite (cube 51) was collected 1000 feet farther south where the strike is east-west and the dip is vertical. The grain size varies greatly in the outcrop and is from 0.05 to 0.40 inches in cross section on the cube's faces. The cube has a few fractures perpendicular to the bedding which are difficult to discern. A thin section shows mostly quartz with much microcline, plagioclase, and orthoclase, with a little muscovite in the fractures.

The white Lorrain quartzite (cube 52) was collected from the summit of Quartz Rock, McGregor Bay Point where the clean white rock is jointed along its bedding planes. The thin beds strike N 75° W, dip 70° N and are cut by a nearly horizontal set of fractures. The cube is diagonally cut by two or three fractures which do not completely cross the cube. A thin section shows 100% quartz.

The banded cherty Lorrain quartzite (cubes 53 and 54) is the youngest metasedimentary rock in this area and was collected in a railroad cut at the west end of Frood Lake. The banding strikes N 80° W and dips 85° N, and the outcrop is cut by several vertical fractures so that finding a

large enough, solid sample was difficult. Cube 53 has distinct fine banding cut by a few healed fractures. The pattern on cube 54 may be entirely due to healed fractures, except for two mutually perpendicular, fresher fractures which appear to be tight.

The next younger lithology has been called the Sudbury or Nipissing gabbro or metagabbro which occurs as large dikes and sills throughout the Sudbury-Espanola area. In this study, it is called "Sudbury gabbro," and samples of it (cubes 55 and 56) were collected from a hilltop road cut 0.5 miles south of Clear Lake.

The extent of the body is very large but undetermined. A faint banding has a strike of N 10° W and a vertical dip. A thin section shows plagioclase, quartz, epidote, abundant fibrous amphibole, and some hornblende. Cube 56 is lighter in color and density than cube 55 and has two healed fractures in it.

Olivine diabase (cubes 57, 58, and 59), commonly called Keweenawan diabase, was collected along Highway 68, 0.2 miles north of Clear Lake where the Sudbury gabbro is cut by a dike of this material. There is no lineation within the dike which strikes N 30° W. Three cubes were cut, none of which has foliation, banding, or fractures. Cube 59 has a corner of predominantly light color while the lithology is normally dark colored. A thin section contains plagioclase, olivine, biotite, pyroxene, apatite, and a few opaques.

An amphilbolite dike ("East dike," cube 60) was sampled from just east of Wanderer's cottage on the north side of the tip of McGregor Bay Point. The dike is 30 feet wide and strikes northwest with a vertical dip. It is black with light colored phenocrysts of feldspar dotting portions of it. It is intruded into the Lorrain quartzite, so it is post-Huronian in age. A thin section is at least half hornblende with indefinite grain boundaries, with epidote, secondary quartz, and some highly altered feldspar.

A second amphibolite dike was sampled just west of Wanderer's cottage (cubes 61, 62, and 63). It is uniformly black, 25 feet wide, strikes north-south and dips 80° E. The two amphibolite dikes are very similiar in appearance and composition except that the second ("West dike"), lacks the altered feldspar. Cubes 61 and 63 were cut from aphanitic samples, and cube 62 from a sample with hornblende crystals up to 0.15 inches in diameter.

A biotite schist (cubes 64 and 65) was collected from a small island (25 x 100 feet) near the crossing of the hydroelectric power lines from the mainland to the southwest side of Iroquois Island, McGregor Bay. This small island, 25 feet from the mainland, is of a variable composition which weathers to a very rough surface. The biotite schist was obtained from depressions a few feet square at the south end of the island. Neither the origin nor the age of this lithology is known. A thin section shows

mostly biotite and quartz with a small amount of chlorite. Cube 65 has more quartz and does not show the foliation seen in cube 64.

Cubes 66 and 67 are from an aplite outcrop near Cutler, Ontario. The aplite is believed to be the chilled margins of the Cutler Granite Batholith, but may be part of a quartzite or graywacke highly altered by the intrusion. The outcrop is along the Lake Huron shore, 0.25 miles southwest from the end of Cutler Bay, and has a 20 foot high navigational target on it. It is about 100 yards south of an old frame church along a dirt driveway. A thin section shows mostly quartz with plagioclase, microcline, and muscovite, and is strongly foliated. The rock was formed during the Killarney Age.

Ordovician limestone (cubes 68 and 69) is the only sedimentary lithology of this study and was collected from the tip of Cloche peninsula as a contrast to the pre-Cambrian metasedimentary and meta-igneous lithologies of this study. The horizontal Ordovician strata at this location have not been metamorphosed. Samples were collected from a fresh road cut 100 yards north of Swift Current. Cube 68 is reddish gray with a few fossil fragments, and cube 69 is greenish gray of heterogeneous composition.

Vein quartz (cube 70) was collected 0.5 miles along an unimproved dirt road west of Highway 68 at the southwest tip of Loon Lake. The vein is at least 200 feet in length

and width but its true extent is obscured by swamp and soil. The cube is 100% pure white quartz with several tight fractures in this brittle material. This vein is probably post-Huronian and occasionally has been quarried.

Lithologies Collected From Other Areas

The Littleton granite gneiss (cube 70) was collected by David Chipman from Crawford Notch, New Hampshire. The cube is heterogeneous and contains a poorly defined, dark zone of biotite parallel to two of the faces. No fractures can be seen. Thin sections show quartz, orthoclase, plagioclase, biotite, and chlorite.

Cubes 72 and 73 of Grenville gneiss were cut from samples collected by Dr. H. Stonehouse from Parry Sound, east of Lake Huron. Because its well developed gneissic texture was expected to cause high anisotropy, two cubes of it were added to this study. The composition is mostly quartz and biotite with smaller amounts of feldspar and hornblende.

Samples of Quincy granite (cubes 74 and 75) were taken from the rock collection of the Geology Department, Michigan State University. It is assumed that this is the same, or very similar to, the granite from Quincy, Massachusetts studied by Birch (1960) and by Hughes and Maurette (1956). Birch gives a composition of 63% albite and microperthite, 26% quartz, and 10% amphibole for the Quincy

granite. Both cubes have very numerous, small, random, closed fractures showing no regard for the grains which are up to 0.3 inches long.

These 73 specimens may be classified into eight lithologic groups. Fourteen specimens are quartzites, seven are granites, five are granite gneiss, eleven are argillites, eight are limestones, eleven are schists, twelve are basic igneous rocks, and five are Negaunee iron formation. The McKim graywacke is described as a micaceous quartzite and is included with the quartzites. The quartz latite porphyry and Cutler aplite are included with the granites. The Siamo slate is considered an argillite and the Kona dolomite is included with the limestones. The serpentinite is placed with the basic igneous classification.

CHAPTER III

PREPARATION OF TEST SPECIMENS

The rock samples collected were taken to the Geology Department, Michigan State University to be cut into cubes approximately two inches on a side. This size is large enough to give typical velocities of the lithologies and small enough to transmit a clear signal. In smaller cubes, a less typical section of the formation might have been sampled, and in cubes very much larger the energy pulse becomes too highly attenuated for accurate measurements with the available instrumentation. When the test specimen is roughly cubical there is no possibility of measuring a "bar velocity," which is a characteristic of the specimen's dimensions and not just the specimen's material. The velocities measured through the cubes are believed to be the true compressional and shear wave velocities.

Of the thirty-five lithologies, eight are represented by one specimen, twenty by two specimens, four by three specimens, two by four specimens, and one by five specimens. There are a total of 73 specimens which required about 200 hours to cut into cubes. Ninety per cent of the cutting was done on a 24 inch diameter slabing saw with an automatic

feed, and the remainder was done on an 8 inch diameter, hand fed saw. The samples usually had banding, bedding, or a fracture pattern which was suspected of causing velocity anisotropy. The cubes were cut with one pair of faces parallel to and two pair perpendicular to any visible structural orientation of the sample, so that the true maximum and minimum velocities would be measured.

Unless the cut faces were smooth with no saw marks on them, they were ground smooth on a lapping wheel with number 180 silicon carbide grit. The same equipment was used to make the opposite sides of the cubes parallel so that five scattered measurements by a calibrated micrometer of the distance between faces agree to within 0.005 inches. The accuracy of the dimension measurements is much greater than that of the travel time measurements, so the uncertainty of the former does not significantly effect the accuracy of the velocity determinations.

CHAPTER IV

DENSITY MEASUREMENTS

The density was determined by weighing the cubes in air on a triple beam balance, and then weighing them while submerged in water. Density is equal to the weight in air divided by the weight-loss-in-water. The "bulk density" also was determined from the weight in air divided by the product of the three dimensions, and is consistantly 0.02 to 0.06 g/cc lower than the first method. The cubes were submerged for about five minutes to wet their surfaces before they were placed on the balance for the submerged weighing. Water soaking into the cubes may cause part of this difference, but not all of it. On cube 9 of serpentinite the total difference (0.056 g/cc) would have to be accounted for by 2.5 cc of water soaking into the volume of 129.1 cc. This would indicate water completely filled a porosity of 1.9% in five minutes. Both the porosity and the time to fill it are unreasonable for serpentinite. In addition, the brass cylinder (2.735 inches X 2.0 inches diameter) has a 0.08 g/cc difference between the methods which can not be accounted for by water filling pore space. The consistant difference between densities measured by these two methods may be

caused by an inaccurate balance or weighing technique. There should not be an inherent difference, but this problem should be studied in greater detail.

"Bulk densities" are easier to determine, and therefore are used in previous studies. However, corners chipped from the cubes erratically effect the "bulk density" values of this study, which makes it necessary to use the densities from the "weight-loss-in-water" method. The density values range from 2.62 g/cc for Serpent quartzite to 3.10 g/cc for olivine diabase and up to 3.67 g/cc for Negaunee iron formation.

After the density measurements were made, a small identification number was painted on the upper right corner of the "front" face of each cube. The "side" and "top" faces are in those respective positions when the "front" face with the number in the upper right corner is facing the observer.

CHAPTER V

ULTRASONIC PULSE MEASUREMENTS

Introduction

The ultrasonic measurement of sound velocity using piezoelectric crystals to convert an electric pulse into mechanical energy has evolved since World War II when the necessary technology and equipment were developed. In 1950 it was first applied to geology. The method has become an accurate means of velocity determination for studies of the characteristic velocity of materials, factors effecting velocity, and "dynamically" determining elastic constants.

Description of Method

The block diagram of the experimental set up is presented in Figure 4. An electrical signal generator produces a pulse which may be in the form of a square wave (all frequencies) or a harmonic sine wave of a single frequency. The frequency, pulse length, pulse amplitude, and repetition rate can be varied by adjusting settings of the instrument. The electrical pulse is sent to the transmitting transducer which changes dimensions when a voltage is applied across it, and thereby converts

electrical to mechanical energy. The mechanical pulse travels through the test specimen at the specimen's characteristic velocity, and upon arrival at the receiving transducer changes its thickness to regenerate the electrical pulse.

The electrical pulse, delayed by its travel through the specimen, is amplified and displayed on an oscilloscope screen. It looks very similiar to a short trace on a conventional seismogram. The first significant motion along the trace is picked as the arrival time of the pulse. The pulse directly from the signal generator is displayed on a separate oscilloscope trace to indicate the instant the pulse started, and its beginning is the "zero time" from which the arrival time is measured. "Zero time" is not necessarily the first vertical line of the grid which is superimposed on the traces for measuring the travel time. For the compressional wave photographs, "zero time" is 0.05 cm. to the right of the vertical line; and it varies on the other photographs. The faces of the transmitting and receiving transducers were placed in contact with each other and showed an immediate rise from zero time. This demonstrates that there is no time delay in the equipment to cause an error in travel time measurements. From the known dimension and travel time, velocity is easily calculated.

Transducers are often made from quartz crystals which have a natural piezoelectric effect. They also can be made from ceramic barium titanite or from newly developed lead zirconate titanate. The ceramic is cooled through its Curie point in a strong magnetic field which leaves the material permanently polarized and having a piezoelectric effect. The faces of the crystal to which the electrical leads are attached determine whether a compressional or shear wave will be generated. If the pulse is applied across the transducer in the direction of polarization, a compressional wave is generated, and a shear wave is generated by applying the pulse perpendicular to this direction of polarization.

The compressional wave transducers used in this study were 1.5 inch diameter lead zirconate titanate discs with a resonate frequency of 370 kcps instead of the 470 kcps specified by the manufacturer. The shear wave transducers were plates (0.25 x 0.25 x 0.12 inches) of the same material which were specified to resonate at 460 kcps. One of these transducers resonated at 360 kcps and the other at 370 kcps, with nearly equal responses at 250 and 260 kcps respectively. The dimensions of these shear transducers were such that the compressional energy generated should have a frequency of about 1 Mcps. One shear transducer resonated slightly at 0.98 Mcps and the other at 1.09 Mcps probably representing the compressional fundamental

frequencies. The resonant points were determined utilizing a Hewlett-Packard Test Oscillator model 650 A.

Experimental Set-Up

The electronic equipment in this study was all calibrated by and loaned from the Bendix Systems Division, Ann Arbor, Michigan.

A Hewlett-Packard Pulse Generator model 212A was used to generate an 80 volt pulse in the form of a square wave, 1.3 μsec. long for the compressional velocity measurements and 2.1 μsec. long for the shear velocity measurements. The pulse was repeated at a rate of approximately 10 times a second, which is the minimum setting on the instrument and which produces the clearest traces on the oscilloscope screen. The oscilloscope is a dual-trace Tektronix, Type 545A Oscilloscope with a Type 53/54C Plug-in Unit Preamplifier, and it is triggered off the output pulse from the signal generator. This same pulse is attenuated 30 decibels before being fed into the oscilloscope's preamplifier and displayed on the upper trace of the screen for timing purposes.

The 80 volt pulse from the pulse generator is applied without attenuation to the transmitting transducer. From this square pulse, the transducer responds to its resonant frequency and vibrates, producing a mechanical sine wave of that frequency. The wave travels through the specimen

and causes the receiving transducer to generate an electrical wave. This wave is fed into the preamplifier and displayed on the lower trace of the screen. For the shear waves a Hewlett-Packard Model 450A Amplifier is added to amplify the very weak received signal by 20 decibels before it is fed into the preamplifier. The sweep speed of the oscilloscope (indicating how much time one centimeter in a horizontal direction represents) is usually set on 2 μsec/cm for compressional velocity measurements and 5 μsec/cm for shear velocity measurements.

Experimental Procedure

The compressional wave velocity measurements were made before the shear velocity measurements and will be discussed first.

The compressional transducers were mounted with "Silastic" in cylindrical holders so as to allow maximum vibration and protection. The "back" face of the test cube was placed down on one transducer, and the second transducer was placed on the "front" face of the cube. A twenty-five pound weight was normally placed on top of this assembly to improve the sharpness of the signal. This also was improved by putting silicon grease on the contact between the specimen and transducer. With the transmitted signal now visible on the screen, the vertical amplification and the trace positions were adjusted, and a photograph

of the screen was taken. The screen grid light was turned off, the input pulse trace was turned off, and the trace showing the pulse transmitted through the specimen was lowered to its middle position. The cube was rotated so that the pulse traveled from one "side" face to the other. A second exposure on the same film was made, and the trace was lowered to its bottom position. The cube again was rotated so that the pulse traveled between the "top" and "botton" faces, and a third exposure was made.

The compressional wave photographs are presented in Figures 5, 6, and 7. The photographs have four traces on them. The input pulse, for timing purposes, is on the top trace, the "front" face measurement on the next trace, the "side" face measurement on the third trace, and the "top" face measurement on the bottom trace. The grid is superimposed over these traces, and is one centimeter between lines on the oscilloscope screen. The film is Polarcid Type 47 with an ASA 3000 equivalent speed. The compressional wave photographs were taken at f5.6 and 1/10 of a second exposure.

The small shear transducers were mounted in holes, cut about 0.1 inch deep into 1/4 inch plywood, to protect them during the measurements and to make them easier to manipulate. It was much more difficult to time the arrival of shear waves than compressional waves although they look identical on the oscilloscope screen. The largest problem

encountered with shear waves was that the shear transducers generated a compressional pulse in addition to the shear pulse. Because compressional waves always travel faster than shear waves, the first break on the trace was the arrival of compressional energy rather than shear energy. This caused the trace to already have considerable motion when the shear pulse arrived, and made picking this arrival very difficult. Other workers have encountered this problem and have had different degrees of success with it. The first arrival was identified as compressional energy when its travel time was close to the previous compressional velocity measurements.

Before a photograph was taken, the clarity of the suspected shear arrival was maximized by adjusting the position of the transducers on the specimen and by adjusting the slight, but unknown, pressure applied by the vise holding the transducers to the specimen. If the cubes had not been coated with silicon grease from the previous compressional velocity measurements, the shear energy might have been increased by cementing the transducers to the specimen so that there could be no slippage between them. This was attempted on the grease coated cubes, but the cement did not hold. Silicon grease is very difficult to remove and therefore no attempt was made to do this.

A second problem was caused by the weak signal arriving at the receiving transducer. The shear transducers

for this study are very small and cannot generate a strong mechanical wave. To help overcome this problem, a 20 decibel amplifier was added to the circuit to amplify the received signal before it was sent to the oscilloscope's amplifier. This increased the amplitude of the signal, but also accentuated the noise problem.

Electromagnetic noise is generated by the electrical circuits in the building and by the test equipment itself. Mechanical vibrations also caused some noise. Under the high amplification, the piezoelectric effect of the transducers occasionally picked up audible noise from conversation and music in the background. Shielding the gold strip leads to the transducers with copper screen greatly reduced the electromagnetic noise. By reversing the leads so that those in contact with the test cube were "ground," and by electrically connecting the "ground" leads to plumbing, the signal-to-noise ratio was improved. The oscilloscope and pulse generator were "grounded" through the electrical network of the building, but this apparently differed from true "ground," and did not permit the optimum measurements. For unknown reasons, the noise also was reduced by a person touching the "ground" connection to the rock specimen. On a few specimens it was necessary to "ground" the cube by wrapping copper foil around the four sides not in contact with the transducer and connecting the foil to "ground." By shielding the transducer leads

and by improving the "ground," most of the noise was removed, The audible noise was seldom noticed and not a real problem. The vise which held the specimen and transducers was placed on a damp sponge to reduce the mechanical vibrations, and they rarely were a problem.

The earlier arrival of the compressional waves, however, was a serious problem in the shear velocity measurements. Because of them, the shear arrivals could not be identified in the three directions for 52 of the 73 specimens, and therefore, shear velocities are calculated for only the remaining 21 cubes. The ratio of shear to compressional velocity for the 21 acceptable shear measurements ranges from 0.53 to 0.67. On the specimens which both Birch (1960, 1961) and Simmons (1964) used for compressional and shear velocity measurements respectively, the range is 0.48-0.67, and Woeber et al. (1963) have a range of 0.54-0.67 for their rocks, and 0.48-0.72 for their minerals. Both the compressional and shear velocities, and the ratio between the two for this study fall in the ranges of other workers.

The method of photography of the shear velocity measurements differs from the compressional velocity measurements in that the exposure is changed to f2.8 at 1/100 second, and the grid light is left on for all three exposures. The input pulse is also shown for each transmitted pulse rather than just one per photograph, and the

sweep speed is changed to 5 μsec/cm. The shear velocity photographs are presented in Figure 8.

Accuracy

The greatest source of error in this study, as in most studies utilizing the ultrasonic pulse technique, is the uncertainty in the exact arrival time of the pulse sent through the test specimen. The oscilloscope trace is straight until the pulse arrives, at which time it is smoothly deflected. The lack of a distinct first break is an inherent problem of this method caused by the smooth form of the sine wave. This problem is reduced by decreasing the wave length (increasing the frequency) which decreases the rise time of the sine wave. The relatively low frequency of the transducers was selected so that the wave length would be longer than the largest grain in the specimens. If the wave length is less than the grain dimensions, scattering of the wave greatly weakens the pulse, and attenuation becomes a major problem.

The wave lengths in this study range from 11 to 18 mm for the compressional waves and 6 to 15 mm for the shear waves. Birch (1960) measured velocities with waves only 2 to 3 mm long and had no attenuation problem. Even with these short wave lengths, his greatest error also was caused by a slow rise time of the oscilloscope trace. The first breaks can be made more distinct by increasing the

vertical amplification of the traces. However, if a study of attenuation is planned, this should not be done because the complete oscillation of the oscilloscope traces would not be recorded.

The ability to duplicate a travel time measurement is demonstrated on the "front" face of cube 1 by four compressional wave measurements in addition to the one in the normal course of experiment (Figure 9, n). The travel time is 9.0 $\pm$0.1 μsec for all five measurements. The velocity through the 2.052 inches is therefore 5.79 $\pm$0.07 km/sec. This is an accuracy of $\pm$1.2% which is typical of the compressional velocities. Nine of the 219 compressional wave arrivals are more uncertain; five of them are picked to $\pm$0.2 μsec and four are picked to $\pm$0.3 μsec. The least accurate compressional velocity is 5.24 $\pm$0.17 which is a 3.1% error. This is the velocity measured on the "side" face of cube 8. The inaccuracy caused by uncertainty in the time of arrival is very rarely greater than 2% which is given as the accuracy of the compressional wave velocities.

In the shear wave measurements, the trace is in motion from the compressional wave when the shear wave arrives, which causes its arrival time to be more uncertain. In most determinations the shear wave arrival is picked to $\pm$0.3 μsec. At a typical velocity of 3.25 km/sec this uncertainty causes a $\pm$0.07 km/sec or 2.2% error, which is

representative of most specimens. Except for one time measurement (cube 5) with an accuracy of ±1.0 μsec which results in an error of 5.3%, the remaining measurements are picked to ±0.5 μsec. The least accurate of these is the "side" measurement on cube 61 which has a velocity of 3.93 ±0.14 km/sec (3.5% error). Only two of the 63 shear velocity measurements are less accurate than 3%, which is given as their accuracy.

Comparison with Metal Standards

The compressional and shear wave velocities of brass and magnesium were measured for the purpose of comparing velocities of this study with the known velocities of these standards. (See Table 1 and Figure 9, a-d.) The brass specimens are cylinders two inches in diameter and have lengths of 2.735, 7.997, and 12.002 inches. The compressional wave velocity of these specimens is 4.44, 4.41, and 4.41 km/sec respectively with an average of 4.42 km/sec. The American Institute of Physics Handbook (Gray, 1963) gives the velocity as 4.70 km/sec, Jamieson and Hoskins (1963) found 4.42 km/sec, Wylie *et al*, (1956) found 4.30 km/sec, and the Handbook of Chemistry and Physics (Hodgeman, 1956) lists 3.50 km/sec which seems quite low compared to the others. The 4.70 km/sec value was determined in 1942 by Birch and may have been measured by less accurate methods. The value of 4.42 km/sec

determined in the present work compares very favorably with the published values.

The shear wave velocities on the short, medium, and long cylinders were 2.32, 1.77, and 2.54 km/sec respectively. Because of the poorly defined arrivals on the records and the large scatter of values, these measurements are believed to be inaccurate, and it is mostly by coincidance that their average of 2.21 km/sec is close to the value of 2.11 km/sec reported in the A.I.P. Handbook, or the value of 2.08 km/sec reported by Jamieson and Hoskins.

The magnesium velocities are determined from two lengths of a rectangular bar so that they can be measured through four distances, 0.75, 1.00, 2.65, and 8.075 inches. The compressional wave velocity through these four distances is 5.52, 5.61, 5.75, and 5.40 km/sec with an average of 5.57 km/sec. Of the reported values the Handbook of Chemistry and Physics again is very low with a value of 4.60 km/sec, the A.I.P. Handbook lists 5.77 km/sec, and Jary Crandall (graduate student, Michigan State University, Physics Department) has found the value to be 5.64 - 5.70 km/sec. The value found in this study is within 4% of the acceptable values.

The shear wave velocities for the four distances are 3.28, 2.95, 3.43, and 3.19 km/sec respectively, with an average of 3.32 km/sec. This is 5.5% higher than the only value found in the literature, 3.05 km/sec in the A.I.P. Handbook.

The compressional wave velocities found in this study are considered to be valid because of the close agreement of the brass and magnesium values with the values reported in the literature. The shear wave photographs of both the brass and magnesium determinations would be classified as unacceptable had they been rock specimens, because of the ambiguous shear arrivals. In addition to weak shear arrivals, the wrong arrival was emphasized during the measurements on five of the seven traces. Had the experimenter known the approximate travel time, the records might have been made clearer by adjusting the amplification or pressure on the transducers. As it is, the shear velocity for brass is considered inaccurate. However, the magnesium shear velocity records do show clear breaks on the traces for the two greatest dimensions. Because of this clarity and because the measured value is only 5.5% different from the only value found in the literature, it is believed that shear wave velocities can be measured when the arrival is clear. This is the case in 21 of the 73 sets of measurements, so only these 21 are analyzed and the remaining 52 are discarded.

Comparison with Specimens From Woeber, Katz, and Ahrens

Five of the specimens studied by Woeber, Katz, and Ahrens (1963) were obtained and their velocities were determined to establish a comparison between the two

studies. (See Table 2 and Figure 9, e-m). The selection of their specimens for the present study was intended to cover a large density range and to use the largest specimens available which is necessary because of the large compressional wave transducers. For the compressional velocity measurements Woeber et al. used a 50 volt sine wave pulse of 0.5 μsec length and 2 Mcps barium titanate transducers, and in the present study an 80 volt square wave pulse, 1.3 μsec. long is used with 0.37 Mcps lead zirconate titanate transducers. For the shear velocity measurements Woeber et al. used a 1500 volt pulse, 10 μsec. long with 2 Mcps "Y" cut quartz transducers and in the present study an 80 volt pulse 2.1 μsec. long is used with 0.26 Mcps lead zirconate titanate transducers. These differences should not cause variation in the velocity measurements made in the two studies. Woeber et al. estimated their values were accurate to 2%, and in the present study the errors of velocity caused by inaccurate picks from the records are rarely greater than 3%.

Except for the kaolin the average compressional wave velocities of the specimens differ by less than 3.5% in the two studies. The velocity of the kaolin in the present study is 29% higher than in the former study. The first breaks are sharp on the record of the present study and do not allow for more than a 1% error. This

studies. (See Table 2 and Figure 9, e-m). The selection of their specimens for the present study was intended to cover a large density range and to use the largest specimens available which is necessary because of the large compressional wave transducers. For the compressional velocity measurements Woeber et al, used a 50 volt sine wave pulse of 0.5 μsec length and 2 Mcps barium titanate transducers, and in the present study an 80 volt square wave pulse, 1.3 μsec. long is used with 0.37 Mcps lead zirconate titanate transducers. For the shear velocity measurements Woeber et al. used a 1500 volt pulse, 10 μsec. long with 2 Mcps "Y" cut quartz transducers and in the present study an 80 volt pulse 2.1 μsec. long is used with 0.26 Mcps lead zirconate titanate transducers. These differences should not cause variation in the velocity measurements made in the two studies. Woeber et al, estimated their values were accurate to 2%, and in the present study the errors of velocity caused by inaccurate picks from the records are rarely greater than 3%.

Except for the kaolin the average compressional wave velocities of the specimens differ by less than 3.5% in the two studies. The velocity of the kaolin in the present study is 29% higher than in the former study. The first breaks are sharp on the record of the present study and do not allow for more than a 1% error. This

rock is very soft and could have been effected by aging during the three years between the two studies,

The shear wave velocity for kaolin is 43% higher in the present study, and is 34% lower for the dacite. These differences probably are due to errors in the present study in picking the shear wave arrivals. The shear wave velocity for the sample of hornblende andesite was not measured, and the values for bytownite and pyrrhotite are only 3 and 7% respectively lower than the values of the former study.

These shear wave velocities were measured when there was still considerable trouble with the experimental setup. Had time permitted, the measurements probably could have been improved after many of the problems had been solved. It is believed that the shear velocity measurements accepted in the main program of this study are more reliable than is indicated by this comparison.

The compressional wave velocities determined by Woeber et al. and in this study compare very well. The shear wave velocity determinations in this study on the specimens from the previous study are inaccurate, but agreed well on two of the four measurements.

CHAPTER VI

RESULTS

Introduction

After the cubes had been cut from the collected samples, and the density and dimensions determined, the travel times in the three directions through the cubes were measured and the velocities were calculated. The results are tabulated in Table 3 and Table 4. The effect of density and fractures on the velocities is considered below, and the elastic constants are calculated and discussed.

Variation of Average Compressional Velocity with Density

To reveal the correlation between compressional wave velocity and density, the average velocity for each cube was calculated and plotted against density (Figure 10). A general increase of velocity with density can be seen, but considering all 73 values, this graph looks like a nearly random scatter of points in the density range of 2.60 to 2.85 g/cc, with a band of nearly equal velocity extending out to a density of 3.10 g/cc, and with a separate group of high density-high velocity values. A much greater correlation of velocity to density had been expected. The studies in the literature had less scatter,

but were usually done under high pressures which closed fractures and produced truer values. However, the graph of this study does have a great deal of order when lithology is considered.

The group of high density-high velocity values are all basic igneous rocks, and no basic igneous rock has a velocity which falls outside this group. The above mentioned band of nearly equal values consists of the schists which increase in velocity from 5.2 km/sec to only 5.5 km/sec over the density range of 2.71 to 3.10 g/cc. The layered Negaunee iron formation extends this band to about 6.5 km/sec at a density of 3.65 g/cc. One cube of biotite schist falls below the band with a velocity of 4.71 km/sec caused by a large anisotropy (36%). If only the average of the two fastest velocities (5.51 km/sec) is plotted, this cube also falls into the schistose band.

In the area of apparent randomness on Figure 10, the argillites are grouped in the higher velocity and density region (6.2 - 6.8 km/sec and 2.91 - 3.10 g/cc). At an equal density, but lower velocity (just above the schistose band) are the two values of Siamo slate. One cube of Espanola argillite (cube 42) is slightly slower and out of the argillite region. However, it is fractured and has a 34% anisotropy. The average of the two velocities parallel to the fractures is 5.87 km/sec which places it in the argillite region. The limestone values are at

an equal velocity, but slightly lower density (2.73 to 2.76 g/cc), except for one cube of Ordovician limestone and one of Espanola limestone. The abnormally low velocities of these two cubes may be due higher porosities. The velocity of the Kona dolomite is high enough to place it in the argillite region. A porosity value smaller than the limestone cubes would cause the dolomite to have a higher velocity. The McKim graywacke is in the limestone region as might be expected, for its composition represents a transition from argillite to quartzite. The low density portion of the graph (2.62 - 2.72 g/cc) is made up of quartzites over a large velocity range (4.88 - 6.22 km/sec) and of granites with lower velocities of 4.08 to 4.81 km/sec. The granite gneisses are scattered slightly on the high density side (up to 2.79 g/cc) of the granites.

When lithology is not considered, the graph shows very poor correlation. But when it is considered, the grouping seems very good, especially when one realizes these are not the true velocity values for these lithologies, which can only be determined under high pressures. Similiar results were obtained by Birch at 10 kilobars pressure. He states that velocity is proportional to density "only within specific subgroups" (Birch, 1961).

Comparison of Anisotropy Determined in Field and Laboratory Studies

In order to study the effect of fractures on velocity, measurements were made on fractured rocks in the field and

non-fractured rocks in the laboratory and the results were compared. Merritt (1961) discovered that on the seven outcrops which he studied, the velocity parallel to the structural orientation (with associated fractures) always was faster than the velocity perpendicular it. The best example of this is the Mona schist which has a velocity of 2.13 km/sec parallel to the structure, and 1.13 km/sec perpendicular to it. For the ultrasonic velocity study, samples were collected from the fractured outcrops of the field study with the intention of obtaining laboratory specimens which have no fractures.

Nine of the 16 cubes have no visible fractures in them. They are one cube of Negaunee iron formation, three cubes of biotite amphibolite schist, two cubes of Mona schist, one cube of serpentinite, and two cubes of granite gneiss. Several of these cubes have healed fractures, not necessarily parallel to the structural orientation, and which do not appear to make the specimen any less solid. Cube 12 of the Negaunee iron formation has a fracture perpendicular to the banding, but it is not visible on one face and leaves the specimen solid. Cube 8 of serpentinite has fractures parallel to all three pairs of faces, and some of the fractures do appear to be open. Cubes 14 and 15 of Siamo slate have a few minor open fractures along the cleavage. While being cut, the slate easily split along its cleavage planes.

Figure 11 compares the velocity anisotropies from the outcrop measurements with those of the laboratory specimens. On the graph the higher end of the velocity range for the cubes is the average of the two velocities parallel to the structure or, where there was none, the average of the two highest velocities. As on the outcrop, the highest velocity is always parallel to the structure. Except for the specimens of biotite amphibolite schist, the field anisotropy always is greater than the laboratory anisotropy. The outcrop of biotite amphibolite schist shows very low anisotropy (2.8%) because the outcrop is "highly contorted" (Merritt, 1961) where the field measurements were made. Over the 70 foot geophone spread, the contortions eliminated the effect of schistocity by equally lowering the velocity in both directions. The laboratory specimens are too small to contain the contortions, and thus show the true anisotropy caused by the schistosity (9.7 - 34%). Omitting this outcrop, the average anisotropy of the outcrops is 40% as opposed to the 13% average for the cubes. The velocities of the laboratory specimens definitely are more isotropic than are the outcrop velocities.

Figure 11 also shows that the velocities of the laboratory specimens consistantly are higher than those of the outcrops, usually by a factor of about two, but by a factor of four in the case of the Mona schist. The

outcrop velocities were measured by standard seismic means and are believed to be correct. The laboratory velocities were measured by a method now accepted as an accurate means of determining velocities, and which gave correct velocities for brass and magnesium in this study. Therefore both the field and laboratory velocities, although very different, are believed to be correct.

Of the factors believed to influence velocity only the lack of solid continuity due to fractures was changed in this comparison, and the above difference is attributed to this factor. The mineral composition, density, porosity, and the size, shape, and orientation of particles in the rock were kept constant. For these metamorphic rocks, the porosity, excluding fractures, is very low, and their fluid content could not have varied significantly. The applied pressure in the laboratory was about 1 bar, and in the field the pressure varied from zero at the surface to an estimated maximum of 35 bars. While a change of pressure, especially at these low pressures, does change the velocity, the sensitivity of velocity to pressure is low enough that the effect would be very slight in this range. If it actually is significant for this small pressure range, it would increase the field velocities and decrease the difference between them and the higher laboratory values. Therefore, the only significant difference between the laboratory and field conditions is the amount of fractures.

The laboratory specimens were especially chosen and cut to eliminate as many fractures as possible, so that they intentionally differ from the outcrops in this respect. The difference between velocities measured in the laboratory and field is attributed to the different number of fractures which energy pulses must pass through or around. In a fractured rock the first energy to be received at the far side of the cube will take the fastest path available, which may be across an air space or a longer path through solid material. The energy will be slowed and attenuated in crossing an air-filled fracture; and, if it takes a solid path longer than the measured thickness, a slower velocity will be calculated. A path through a water-filled fracture also will cause a slower velocity, but not to the extent of an air-filled fracture. Thus, all breaks in the solid continuity of a rock will decrease the velocity measured from it, and the more breaks it has, the slower the velocity will be.

In the velocity measurements on cubes with open fractures, it was often difficult or impossible to obtain a sharp first break of the trace (see photographs of cubes 8, 15, 16, 17, 42, and 49 on Figures 5 and 6. The normal smooth wave form also was destroyed by the open fractures. In this manner, the effect of an open fracture was made very obvious during the laboratory work. Except for the gneisses and schists, it also was these cubes which had

the most extreme anisotropies. Several test cubes have one or two tight fractures which caused no difficulty in obtaining a clear first break. However, these fractures caused a relatively slow velocity for the pulse crossing them. For example, the two or three tight fractures in the otherwise homogeneous cube 52, white Lorrain quartzite, did not interfere with the measurements or distort the wave form, but they are the only explanation for the 17% anisotropy of this specimen. When a fracture is filled with cement, solid continuity is restored and the wave travels unimpeded at the characteristic velocity of the material. The basalt specimen (cube 22) has 3 or 4 cemented fractures, and the velocities perpendicular and parallel to them are equal (anisotropy of 0.78%) within the accuracy of these measurements. Cube 56 has one healed fracture and an anisotropy of 1.3%, and cube 63 also has one healed fracture with an anisotropy of 0.8%. Cemented fractures have no effect, but both open and tight fractures cause a decrease in velocity.

The minute intersticies between a grain and the matrix or cement of a rock are also thought to slow down a pulse of energy. Birch (1960), found 6.8% anisotropy on the Cambridge slate at 10 kilobars confining pressure, and attributed it to the anisotropy within oriented crystals (mostly mica in his discussion) because he assumed all fractures had been closed. However, Walsh (1965) later

showed that, "this behavior [anisotropy of slate] can be explained by assuming that the crystalline framework of the rock is elastic and isotropic but that the distribution of cracks is anisotropic," Thus the anisotropy Birch and other workers have measured at high pressures may have been due to minute interstices around the mineral grains of the rock. The anisotropy of single crystals of mica and clay minerals is unknown, so the cause of anisotropy at high pressures cannot definitely be attributed to either anisotropy within the particles or to the minute fractures surrounding them. The literature is well agreed that all types of solid discontinuity will slow down a pulse of energy, and that this effect can be, at least partially, eliminated by applying enough pressure to make the solid continuous. If all fractures in a specimen are closed and anisotropy still remains, then it must be caused by other factors, such as the anisotropy within the oriented particles composing the rock.

Compressional Wave Anisotropy of all Laboratory Specimens

Figure 12 shows the distribution of anisotropy of the 73 specimens classified into eight lithologic groups. The basic igneous rocks are the most isotropic, with velocity anisotropy values of 3% or less, except for a 12% value which is from the fractured and metamorphosed serpentinite cube. As one would expect, the schists and granite

gneisses show large anisotropy with values up to 36% and 38% respectively, although four of the five granite gneisses are grouped around 13%. The argillites show the greatest anisotropy, but all five values greater than 9% (17% - 34%) are from cubes with open fractures in them. The five cubes of argillite with values less than 9% are all banded, but have no visible fractures. This illustrates quite well the velocity reducing effect of open fractures, and the lack of a large effect due to banding. The limestones have a range from 6% to 15%, and the granites range from 2% to 16%. The quartzite group has a fairly wide range of 1% to 17%. The white Lorrain quartzite and vein quartz are the purest quartz specimens of this study with impurities of less than 0.5%, yet the former has the highest quartzite value (17%), and the latter has a value of 12%. The high anisotropy values, expressing large velocity differences, again are attributed to fractures which are seen in both cubes. The purity of the quartzite group varies from the above cubes down to the McKim graywacke which is about 70% fine quartz and 30% muscovite and chlorite. All the quartzite cubes with values above 6% show fractures or are bedded with a strong possibility of oriented microfractures parallel to the bedding.

The argillites are the most anisotropic specimens of this study, but this is caused by their open fractures and

not by their lithology. The schists are the most anisotropic specimens which have no visible fractures, but probably contain many oriented microfractures. In contrast the basic igneous rocks are very nearly isotropic.

Elastic Constants

The elastic constants are defined in terms of strain produced in a material by an applied stress, (e.g. Dobrin, 1960). Young's modulus (E) is a proportionality constant relating compressive stress (S) to the resulting strain (ε); $S = E\varepsilon$. Poisson's ratio (σ) is the ratio of strain ($\Delta w/w$) perpendicular to a compressive stress to the strain ($\Delta l/l$) parallel to the stress; $\sigma = \frac{\Delta w/w}{\Delta l/l}$, where "w" is width and "l" is length. The shear modulus (μ) is a proportionality constant relating shear stress (S) to the resulting strain represented by the angle ϕ; $S = \mu\phi$. If a body is uniformly compressed in all directions, its volume (V) will be decreased by ΔV. The bulk modulus (K) is a proportionality constant between the applied stress and the proportional change in volume; $S = K \frac{\Delta V}{V}$.

Lame's constant (λ) is defined as $\frac{\sigma E}{(1-2\sigma)(1+\sigma)}$, and it can be shown that, $\mu = \frac{E}{2(1+\sigma)}$. The compressional velocity (V_p) and the shear velocity (V_S) are related to these two constants and density (ρ) by the following equations:

$V_P = \sqrt{\frac{\lambda+2\mu}{\rho}}$, and $V_S = \sqrt{\frac{\mu}{\rho}}$. The identities used to calculate the elastic constants in this study are as follows: $\lambda = \rho(V_P^2 - 2V_S^2)$, $\mu = \rho(V_S^2)$, $\sigma = \frac{\lambda}{2(\lambda+\mu)}$, $K = \lambda + \frac{2}{3}\mu$, and $E = 2\mu(1+\sigma)$. The values are given in Table 5.

Density has a negligible error, the compressional velocity has a 2% error, and the shear velocity has a 3% error. The inaccuracy of these velocities causes errors in the elastic constants as follows: Lame's constant 6%, shear modulus 6%, Poisson's ratio 12%, bulk modulus 12%, and Young's modulus 18%.

The plots of these five constants and of the two velocities against density (Figures 13, 14, 15, 16, 17, 18, and 19) show a considerable scatter of values. Because of this wide scatter, first degree least square lines were computed on the Control Data Computer 3600 and are drawn on the graphs. Most of the scatter is attributed to the fact that the velocities (and therefore, the constants) are dependent not only upon density, but also lithology. This is shown on Figure 10 comparing average compressional velocity with density for all 73 specimens, which separates them into lithologic groups. This agrees with Birch's results that compressional wave velocity depends on both the density and mean atomic weight (Birch, 1961). A smaller part of the scatter is caused by differences between fractured and solid specimens, and by errors in the measurements.

For the 21 specimens on which shear velocities were obtained, the least squares lines of the two velocities and five elastic moduli increase with density. The rate of increase of the compressional velocity is 3.07 km/sec per g/cc, and the shear velocity increases at a much slower rate of 0.94 km/sec per g/cc. The elastic constants increase with density at the following rates: Lame's constant, 77 x 10^{10} dynes/cm^2 per g/cc; shear modulus, 29 x 10^{10} dynes/cm^2 per g/cc; Poisson's ratio, 0.21 per g/cc; bulk modulus, 94 x 10^{10} dynes/cm^2 per g/cc; and Young's modulus, 84 x 10^{10} dynes/cm^2 per g/cc.

It was anticipated that the least square lines would indicate an increase in the physical property with density but, except for compressional velocity, the rates of increase were reported only by Woeber et al. (1963). The rates of compressional and shear velocity, bulk modulus, and shear modulus can be taken from their graphs, but these are for values over a larger density range (1.38 - 3.25 g/cc) and show considerable scatter. Because these plots are not straight lines and are based on a larger density range than those of the present study, the rates cannot be compared in detail. Their rates for shear velocity and, therefore shear modulus are about twice this study's rates, but would probably be lowered if only the values in the density range of the present study were used. Their rate of increase in bulk modulus is about 20%

greater than the rate for this study. Their rate of increase in compressional velocity in the density range of the present study is about the same as this study's and Birch's, which are considered in the following paragraph.

Birch (1961) studied the increase of compressional velocity with density, and found that, if the mean atomic weight remained constant (approximately 21), velocity increased at the rate of 3.05 km/sec per g/cc for 45 silicate rocks at 10 kilobars. This agrees favorably with the 3.07 km/sec per g/cc rate of the present study. Birch accepts an increase of 3 km/sec per g/cc as a typical average for a constant mean atomic weight. By comparison with his chart of mean atomic weights of rocks, the value for the present study probably stayed within the range of 20.6 to 22.0 when the cubes of Negaunee iron formation are excluded. Thus the increase of compressional wave velocity with density found in this study agrees very well with Birch's results at 10 kilobars pressure.

CHAPTER VII

SUMMARY

The ultrasonic pulse technique is used to determine the velocity of compressional and shear waves in three mutually perpendicular directions through cubical laboratory specimens. The validity of these measurements is established by determining the velocities of metal standards, and by duplicating a portion of a previous study.

In this study it is demonstrated that:

1. The 73 specimens studied can be separated into eight distinct lithologic groups on the basis of their compressional velocity and density. The ranges of values for the groups are as follows:

Lithologic Group	Density (g/cc)	Velocity (km/sec)
basic igneous	2.91 - 3.10	6.20 - 6.80
schist	2.71 - 3.10	5.20 - 5.50
iron formation	3.05 - 3.67	5.70 - 6.40
argillite	2.78 - 2.84	5.50 - 6.15
limestone	2.73 - 2.76	5.55 - 6.10
quartzite	2.62 - 2.72	4.90 - 6.20
granite	2.64 - 2.66	4.10 - 4.80
grahite gneiss	2.71 - 2.79	4.20 - 5.00

2. The velocities determined from the laboratory specimens are from two to four times greater than velocities measured in the field by standard seismic techniques. The former have an average anisotropy of 13% compared to 40% for the latter. Both the slower velocities and the higher anisotropies of the outcrops are attributed to a greater degree of fracturing.

3. The anisotropy of the laboratory specimens ranges from 1% to 36%. The fractured specimens are the most anisotropic. Of the non-fractured specimens, the schists and the gneisses are the most anisotropic, and the most isotropic are the basic igneous rocks.

4. Compressional wave velocity of 21 specimens increases with density at a rate of 3.07 km/sec per g/cc which is nearly identical to the rate found in the only previous study (Birch, 1961). The shear wave velocity increases with density at a rate of 0.94 km/sec per g/cc. The rate of increase of Lame's constant with density is 77×10^{10} dynes/cm^2 per g/cc, and the rate for the shear modulus is 29×10^{10} dynes/cm^2 per g/cc. Poisson's ratio has a rate of 0.21 per g/cc, and the bulk modulus has a rate of 94×10^{10} dynes/cm^2 per g/cc. The rate of increase of Young's modulus with density is 84×10^{10} dynes/cm^2 per g/cc.

CHAPTER VIII

RECOMMENDATIONS FOR FUTURE INVESTIGATIONS

The correlation of laboratory and field velocities could be extended by measuring velocities on many of the outcrops from which laboratory samples were collected, but which were not included in the field study.

In areas thinly covered by unconsolidated material, it should be possible to determine the orientation of vertical bedding or jointing pattern in the bedrock, and perhaps to identify the lithology on the basis of its velocity and anisotropy. Merritt (1961) measured 35% anisotropy for the Siamo slate buried under 12 feet of glacial drift, but having a known strike and dip. This problem should be investigated further.

The present study could be extended by determining the shear velocities for the remaining 52 cubes, so that elastic constants could be calculated for all 73 specimens. This would permit a more accurate determination of their correlation with density and lithology.

The "static" elastic constants for these cubes could be measured and compared with the "dynamic" constants found in this study. The constants of rocks determined by these two methods have not been compared.

The effect of fluid content, temperature, and pressure could be studied on these non-homogeneous specimens as it has been for homogeneous specimens.

Other physical properties such as hardness, magnetic susceptibility, and electrical conductivity can be determined and correlated with the properties measured in this study.

In this study a consistant difference between two methods of density determination was noticed. The difference may be due to water seeping into the cubes, but it should be more thoroughly studied and its cause definitely determined.

It is recommended that all future studies use only the metric system and that anisotropy be expressed as $\frac{V_{max_{ave}} - V_{min}}{V_{ave}} \times 100$ to be consistant with the literature. The shear wave measurements might be improved by removing the silicon grease from the cubes and cementing larger transducers onto them. The measurements also might be improved by applying a sine wave pulse of the shear wave frequency to the transmitting transducer. This would largely eliminate compressional waves of other frequencies which can be generated by applying a square wave. To obtain a sharp first break, the vertical amplification of the oscilloscope should be set on the maximum allowed by the noise level for a clear photograph.

REFERENCES CITED

Birch F. 1960. The Velocity of Compressional Waves in Rocks to 10 Kilobars, Part 1. J. Geophys. Res., Vol. 65, 1083-1102.

_____. 1961. The Velocity of Compressional Waves in Rocks to 10 Kilobars, Part 2. J. Geophys. Res., Vol. 66, 2199-2224.

Brace, W. F. 1965. Some New Measurements of Linear Compressibility of Rocks. J. Geophys. Res. Vol. 70, 391-398.

Dobrin, M. B. 1960. Introduction to Geophysical Prospecting. 2nd edition. New York: McGraw-Hill Book Co.

Gray, D. E. (ed.). 1963. American Institute of Physics Handbook. 2nd edition. New York: McGraw-Hill Book Co.

Hodgeman, C. D. (ed.). 1956. Handbook of Chemistry and Physics. Vol. 38. Cleveland, Ohio: Chemical Rubber Publ. Co., 3206 pp.

Hughes, D. S., and Jones, H. J. 1950. Variation of Elastic Moduli of Igneous Rocks with Temperature and Pressure, Bull. Geol. Soc. Am. Vol. 61, 843-856.

Hughes, D. S., and Cross, J. H. 1951. Elastic Wave Velocity in Rocks, Geophysics. Vol. 16, 577-593.

Jamieson, J. C. and Haskins, H. 1963. The Measurement of Shear Wave Velocity in Solids Using Uniaxially Polarized Ceramic Transducers. Geophysics. Vol. 28, 87-90.

Merritt, D. W. 1961. Velocity Anisotropy Studies of Precambrian Lamellar Formations. unpublished Master of Science degree thesis, Michigan State University.

Peselnick, L. and Outerbridge, W. F. 1961. Internal Friction in Shear and Shear Modulus of Solenhofen Limestone over a Frequency Range of 10^7 c/s. J. Geophys. Res. Vol. 67, 581-588.

Peselnick, L. 1962. Elastic Constants of Solenhofen Limestone and Their Dependance on Density and Saturation. J. Geophys. Res. Vol. 67, 4441-4448.

Quirke, T. T. 1917. Espanola District, Ontario. Geol. Surv., Canada, Memoir 102.

Simmons, G. 1964. Velocity of Shear Waves in Rocks to 10 Kilobars, 1. J. Geophys. Res. Vol. 69, 1123-1130

Tocher, D. 1957. Anisotropy of Rocks Under Simple Compression, Trans. A.G.U. Vol. 38, 89-94.

Van Hise, C. R., and Leith C. K. 1911. The Geology of the Lake Superior Region, U. S. Geol. Survey. Monograph 52.

Walsh, J. B. 1965. The Effect of Cracks on the Compressibility of Rocks. J. Geophys. Res. Vol. 70, 381-389.

Woeber, A. F., Katz, S. and Ahrens, T. J. 1963. Elasticity of Selected Rocks and Minerals. Geophysics. Vol. 28, 658-663.

Wyllie, R. J., Gregory, A. R. and Gardner, G. H. F. 1956. Elastic Wave Velocities in Porous Media. Geophysics. Vol. 21, 41-70.

_____. 1958. An Experimental Investigation of Factors Affecting Elastic Wave Velocities in Porous Media. Geophysics. Vol. 23, 459-493.

Zisman, W. A. 1933. Comparison of the Statically and Seismically Determined Elastic Constants of Rock. Proc. Nat'l. Acad. Sci. U. S. Vol. 19, 680-686.

TABLE 1.--Comparison of velocities from metal standards.

Brass			Magnesium		
V_P(km/sec)	V_S(km/sec)	ref.	V_P(km/sec)	V_S(km/sec)	ref.
4.42	2.21	1	5.57	3.32	1
4.70	2.11	2	5.77	3.05	2
4.42	2.08	3	4.60		5
4.30		4	5.65-5.70		6
3.50		5			

References:

1. This study
2. American Institute of Physics Handbook (Gray, 1963)
3. Jamieson and Hoskins (1963)
4. Wyllie, Gregory, and Gardner (1956)
5. Handbook of Chemistry and Physics (Hodgman, 1956)
6. Crandall (1965)

TABLE 2.--Comparison of velocities from specimens of Woeber, Katz, and Ahrens.

Lithology	Woeber ref. no.	V_P(km/sec)			V_S(km/sec)		
		This Study	Woeber et al.	% diff.	This Study	Woeber et al.	% diff.
Kaolin	33	1.56	1.21	+29	1.38	0.93	+43
Hor. And.	2	2.70	2.58	+ 2.1	--	--	--
Dacite	11	5.98	6,12	- 2.3	2.32	3.53	-34
Bytownite	43	6.55	6.78	- 3.4	3.26	3.37	- 3
Pyrrhotite	37	4.59	4.60	- 0.2	2.48	2.66	- 7

TABLE 3.--Principal facts of specimens and compressional wave measurements.

Lithology	Cube No.	Density g/cc	Face*	Dimen. Inch	Time μsec	V_P km/sec	$\Delta V/V_{ave}$ per cent
Negaunee iron formation	1	3.67	f	2.052	9.0	5.79	
			s	1.948	8.6	5.40	
			t	2.018	8.8	5.68	
			ave			5.79	1.2
Negaunee iron formation	2	3.05	f	2.020	9.1	5.64	
			s	2.083	9.3	5.69	
			t	2.029	10.6	4.86	
			ave			5.40	15.4
Negaunee iron formation	3	3.52	f	1.822	7.8	5.93	
			s	2.138	9.2	5.90	
			t	1.992	9.7	5.22	
			ave			5.68	12.6
biotite amphibole schist	4	2.88	f	1.867	11.3	4.20	
			s	2.045	8.7	6.00	
			t	2.045	9.1	5.71	
			ave			5.30	34.0
biotite amphibole schist	5	2.95	f	2.045	10.4	4.99	
			s	2.017	9.3	5.51	
			t	1.736	8.1	5.44	
			ave			5.32	9.7
biotite amphibole schist	76	2.95	f	1.976	8.9	5.64	
			s	2.009	9.3	5.49	
			t	1.991	10.6	4.77	
			ave			5.30	16.4
Mona schist Lt. House Point	6	2.94	f	2.050	8.2	6.35	
			s	1.913	7.2	6.75	
			t	2.014	7.6	6.73	
			ave			6.61	6.0
Mona schist Lt. House Point	7	3.04	f	2.048	7.5	6.94	
			s	1.973	7.3	6.86	
			t	2.021	8.3	6.18	
			ave			6.66	11.3
Serpentin.	8	2.74	f	2.059	11.3	4.63	
			s	1.959	9.5	5.24	
			t	2.032	10.4	4.96	
			ave			4.94	12.3

Lithology	Cube No.	Density g/cc	Face*	Dimen. Inch	Time μsec	V_P km/sec	$\Delta V/V_{ave}$ per cent
Serpentin	9	2.87	f	2.000	9.1	5.58	
			s	2.017	9.3	5.51	
			t	1.953	9.0	5.51	
			ave			5.54	1.3
granite gneiss	10	2.71	f	2.026	9.6	5.36	
			s	2.015	10.4	4.92	
			t	2.089	11.4	4.66	
			ave			4.98	14.1
granite gneiss	11	2.71	f	2.060	10.8	4.84	
			s	2.039	9.8	5.29	
			t	1.907	10.9	4.44	
			ave			4.86	17.3
Negaunee iron formation	12	3.58	f	2.022	8.4	6.12	
			s	2.052	8.3	6.28	
			t	1.987	8.3	6.08	
			ave			6.16	1.0
Negaunee iron formation	13	3.62	f	2.128	8.3	6.52	
			s	2.028	7.9	6.52	
			t	1.796	7.4	6.16	
			ave			6.40	5.5
Siamo slate	14	2.79	f	1.599	8.5	4.78	
			s	2.026	8.8	5.85	
			t	1.924	8.6	5.68	
			ave			5.44	19.6
Siamo slate	15	2.84	f	2.031	8.9	5.80	
			s	1.979	8.5	5.91	
			t	2.009	11.5	4.44	
			ave			5.38	27.4
Mona schist Chocolay	16	2.73	f	1.974	12.0	4.18	
			s	2.090	9.1	5.84	
			t	1.945	8.6	5.75	
			ave			5.25	31.5
Mona schist Chocolay	17	2.74	f	1.954	8.8	5.64	
			s	2.021	9.1	5.64	
			t	1.934	11.5	4.27	
			ave			5.18	26.4
Mesnard quartzite	18	2.66	f	1.799	7.7	5.94	
			s	1.665	7.2	5.88	
			t	1.865	8.2	5.78	
			ave			5.86	2.7

Lithology	Cube No.	Density g/cc	Face*	Dimen. Inch	Time μsec	V_P km/sec	$\Delta V/V_{ave}$ per cent
Mesnard quartzite	19	2.67	f	2.060	9.0	5.82	
			s	2.017	8.7	5.89	
			t	1.910	8.3	5.85	
			ave			5.85	1.2
Kona dolomite	20	2.81	f	2.006	9.5	5.37	
			s	2.041	8.3	6.25	
			t	2.092	8.6	6.18	
			ave			5.93	14.8
Kona dolomite	21	2.81	f	2.010	8.5	6.01	
			s	2.032	9.5	5.43	
			t	2.006	8.7	5.86	
			ave			5.77	10.0
basalt	22	2.91	f	1.933	7.4	6.64	
			s	1.975	7.5	6.69	
			t	1.972	7.5	6.68	
			ave			6.67	0.8
quartz latite porphyry	23	2.68	f	2.010	8.5	6.01	
			s	1.995	8.4	6.03	
			t	1.977	8.9	5.64	
			ave			5.90	6.6
amphibole biotite schist	24	3.06	f	1.930	10.3	4.76	
			s	2.002	9.2	5.53	
			t	1.977	8.1	6.20	
			ave			5.50	26.2
amphibole biotite schist	25	3.10	f	2.060	8.6	6.08	
			s	1.978	8.9	5.65	
			t	2.000	10.9	4.66	
			ave			5.46	26.0
Republic granite	26	2.63	f	2.045	11.9	4.36	
			s	2.008	11.8	4.32	
			t	1.985	11.8	4.27	
			ave			4.32	2.2
Republic granite	27	2.63	f	2.054	11.1	4.70	
			s	2.089	12.0	4.42	
			t	2.002	11.6	4.38	
			ave			4.50	7.0
McKim graywacke	31	2.76	f	1.969	9.5	5.27	
			s	2.025	8.9	5.78	
			t	2.023	8.5	6.04	
			ave			5.70	13.6

Lithology	Cube No.	Density g/cc	Face*	Dimen. Inch	Time μsec	V_P km/sec	$\Delta V/V_{ave}$ per cent
McKim graywacke	32	2.79	f	2.035	8.8	5.88	
			s	1.929	8.8	5.57	
			t	2.013	8.0	6.39	
			ave			5.94	13.8
Mississ. quartzite	33	2.68	f	1.956	9.6	5.18	
			s	2.040	9.5	5.45	
			t	1.908	8.8	5.51	
			ave			5.38	6.2
Mississ. quartzite	34	2.68	f	2.035	10.4	4.97	
			s	1.912	9.4	5.17	
			t	2.015	10.9	4.70	
			ave			4.94	9.5
Espanola limestone	35	2.74	f	1.994	8.7	5.82	
			s	1.953	8.9	5.57	
			t	2.032	9.7	5.32	
			ave			5.57	8.9
Espanola limestone	36	2.74	f	1.856	8.0	5.89	
			s	2.058	8.6	6.08	
			t	1.997	8.1	6.26	
			ave			6.08	6.1
Espanola limestone	37	2.73	f	2.016	8.3	6.17	
			s	1.998	8.5	5.97	
			t	1.977	8.8	5.71	
			ave			5.95	7.8
Espanola limestone	38	2.71	f	2.024	10.9	4.72	
			s	1.865	10.8	4.39	
			t	1.898	11.9	4.05	
			ave			4.39	15.2
Espanola argillite	39	2.83	f	2.051	8.5	6.13	
			s	2.002	8.3	6.13	
			t	1.862	8.2	5.77	
			ave			6.01	6.0
Espanola argillite	40	2.80	f	1.931	8.3	5.91	
			s	2.043	8.7	5.97	
			t	2.036	9.0	5.75	
			ave			5.88	3.7
Espanola argillite	41	2.83	f	1.919	8.5	5.74	
			s	1.992	8.5	5.95	
			t	1.812	8.0	5.76	
			ave			5.82	3.7

Lithology	Cube No.	Density g/cc	Face*	Dimen. Inch	Time μsec	V_P km/sec	$\Delta V/V_{ave}$ per cent
Espanola argillite	42	2.87	f	1.848	8.0	5.87	
			s	1.891	8.2	5.86	
			t	1.930	12.0	4.08	
			ave			5.27	33.8
Serpent quartzite	43	2.62	f	1.974	10.1	4.96	
			s	1.973	10.2	4.91	
			t	1.970	10.5	4.76	
			ave			4.88	4.1
Serpent quartzite	44	2.63	f	1.819	9.2	5.02	
			s	2.041	9.9	5.24	
			t	1.798	8.9	5.13	
			ave			5.13	4.2
Gowganda argillite	45	2.84	f	2.097	9.3	5.73	
			s	2.022	8.2	6.26	
			t	1.932	8.4	5.84	
			ave			5.94	9.0
Gowganda argillite	46	2.79	f	1.822	7.8	5.94	
			s	2.001	8.0	6.35	
			t	1.771	7.7	5.84	
			ave			6.04	8.4
Gowganda argillite	47	2.79	f	1.970	8.1	6.18	
			s	1.634	7.4	5.61	
			t	1.498	5.7	6.68	
			ave			6.16	17.3
Gowganda argillite	48	2.73	f	1.888	8.0	6.00	
			s	2.021	8.4	6.12	
			t	2.020	8.5	6.04	
			ave			6.05	2.0
Gowganda argillite	49	2.80	f	1.998	8.1	6.27	
			s	2.043	8.9	5.83	
			t	1.905	11.0	4.40	
			ave			5.50	34.0
gray Lorrain quartzite	50	2.71	f	2.019	9.0	5.70	
			s	2.020	8.4	6.11	
			t	1.807	8.8	5.22	
			ave			5.67	15.7
pink Lorrain quartzite	51	2.65	f	1.917	9.9	4.92	
			s	2.000	10.0	5.08	
			t	1.999	10.0	5.08	
			ave			5.03	3.3

Lithology	Cube No.	Density g/cc	Face*	Dimen. Inch	Time μsec	V_P km/sec	$\Delta V/V_{ave}$ per cent
white Lorrain quartzite	52	2.64	f	2.014	9.5	5.39	
			s	1.911	9.1	5.34	
			t	2.149	12.1	4.51	
			ave			5.08	17.2
banded Lorrain quartzite	53	2.68	f	2.001	8.4	6.05	
			s	2.056	8.5	6.15	
			t	1.931	8.6	5.70	
			ave			5.97	7.4
banded Lorrain quartzite	54	2.72	f	1.956	8.3	5.99	
			s	1.925	9.3	5.26	
			t	1.959	8.0	6.22	
			ave			5.82	16.5
Sudbury gabbro	55	3.05	f	2.027	7.7	6.68	
			s	1.980	7.5	6.71	
			t	2.028	7.8	6.61	
			ave			6.67	1.5
Sudbury gabbro	56	2.99	f	1.879	7.3	6.54	
			s	2.108	8.3	6.45	
			t	1.922	7.5	6.51	
			ave			6.50	1.3
olivine diabase	57	3.10	f	1.991	8.1	6.24	
			s	1.998	8.1	6.27	
			t	2.038	8.5	6.09	
			ave			6.20	2.8
olivine diabase	58	3.02	f	1.961	7.9	6.30	
			s	1.961	7.9	6.30	
			t	2.035	8.4	6.16	
			ave			6.26	2.4
olivine diabase	59	3.01	f	1.966	8.0	6.24	
			s	1.982	8.2	6.14	
			t	1.972	8.1	6.18	
			ave			6.19	1.7
east amphibole dike	60	2.99	f	2.099	8.0	6.67	
			s	2.018	7.7	6.66	
			t	2.056	7.9	6.61	
			ave			6.65	0.9
west amphibole dike	61	3.09	f	2.052	7.8	6.68	
			s	2.014	7.6	6.73	
			t	2.037	7.6	6.81	
			ave			6.74	1.8

Lithology	Cube No.	Density g/cc	Face*	Dimen. Inch	Time μsec	V_P km/sec	$\Delta V/V_{ave}$ per cent
west amphibole dike	62	3.08	f	1.982	7.4	6.81	
			s	2.054	7.9	6.61	
			t	2.008	7.6	6.71	
			ave			6.71	3.0
west amphibole dike	63	3.07	f	1.976	7.4	6.78	
			s	1.997	7.5	6.76	
			t	1.826	6.8	6.82	
			ave			6.79	0.8
biotite schist	64	2.81	f	1.809	12.0	3.83	
			s	1.849	8.5	5.52	
			t	1.752	9.3	4.79	
			ave			4.71	36.0
biotite schist	65	2.71	f	2.002	9.2	5.52	
			s	1.932	9.6	5.11	
			t	2.005	10.0	5.09	
			ave			5.24	8.2
Cutler aplite	66	2.66	f	1.998	11.1	4.57	
			s	1.957	10.5	4.73	
			t	1.998	9.9	5.13	
			ave			4.81	11.5
Cutler aplite	67	2.66	f	2.021	11.9	4.31	
			s	2.024	11.1	4.63	
			t	2.018	10.1	5.10	
			ave			4.64	16.3
Ordovician limestone	68	2.69	f	1.991	10.5	4.82	
			s	1.991	10.4	4.86	
			t	1.853	11.3	4.17	
			ave			4.62	15.0
Ordovician limestone	69	2.76	f	2.105	9.4	5.69	
			s	2.030	9.0	5.73	
			t	2.063	9.6	5.46	
			ave			5.63	4.8
vein quartz	70	2.64	f	1.673	6.8	6.25	
			s	1.817	7.9	5.84	
			t	1.962	7.6	6.56	
			ave			6.22	11.5
Littleton granite gneiss	71	2.72	f	1.952	10.8	4.59	
			s	1.931	11.8	4.16	
			t	1.891	10.3	4.66	
			ave			4.47	11.4

Lithology	Cube No.	Density g/cc	Face*	Dimen. Inch	Time μsec	V_P km/sec	$\Delta V/V_{ave}$ per cent
Grenville granite gneiss	72	2.76	f	2.006	10.6	4.81	
			s	1.991	12.1	4.18	
			t	1.926	10.9	4.49	
			ave			4.49	14.0
Grenville granite gneiss	73	2.79	f	2.041	10.2	5.08	
			s	1.980	12.4	4.06	
			t	1.965	14.3	3.49	
			ave			4.21	37.9
Quincy granite	74	2.65	f	2.042	13.7	3.79	
			s	1.989	11.9	4.24	
			t	1.993	12.0	4.22	
			ave			4.08	11.2
Quincy granite	75	2.65	f	2.026	12.2	4.25	
			s	2.027	12.0	4.29	
			t	1.983	12.4	4.06	
			ave			4.20	5.4

* f = front
s = side
t = top

TABLE 4.--Principal facts of specimens and shear wave measurements.

Lithology	Cube No.	Density g/cc	Face*	Dimen. Inch	Time μsec	V_s km/sec
Negaunee iron formation	2	3.05	f	2.020	16.0	3.21
			s	2.083	17.0	3.11
			t	2.029	13.6	3.79
			ave			3.37
biotite amphibole schist	5	2.95	f	2.045	16.5	3.15
			s	2.017	15	3.42
			t	1.736	13.5	3.27
			ave			3.28
serpentin.	9	2.87	f	2.000	15.0	3.39
			s	2.017	15.0	3.42
			t	1.953	13.2	3.76
			ave			3.52
Mesnard quartzite	19	2.67	f	2.060	15.8	3.31
			s	2.017	14.6	3.51
			t	1.910	13.7	3.54
			ave			3.46
Espanola argillite	42	2.87	f	1.848	17.2	2.73
			s	1.891	16.8	2,86
			t	1.930	17.8	2.75
			ave			2.78
Serpent quartzite	43	2.62	f	1.974	16.8	2.98
			s	1.973	16.4	3.05
			t	1.970	16.5	3.03
			ave			3.02
Serpent quartzite	44	2.63	f	1.819	16.3	2.84
			s	2.041	14.5	3.58
			t	1.798	14.0	3.26
			ave			3.22
Sudbury gabbro	56	2.99	f	1.879	16.5	2.89
			s	2.108	16.0	3.35
			t	1.922	17.3	2.82
			ave			3.02
olivine diabase	57	3.10	f	1.991	14.3	3.54
			s	1.998	13.0	3,90
			t	2.038	13.8	3.75
			ave			3.73

Lithology	Cube No.	Density g/cc	Face*	Dimen. Inch	Time μsec	V_s km/sec
olivine diabase	58	3.02	f	1.961	13.8	3.61
			s	1.961	15.0	3.32
			t	2.035	14.7	3.52
			ave			3.48
olivine diabase	59	3.01	f	1.966	15.0	3.33
			s	1.982	14.3	3.52
			t	1.972	13.6	3.68
			ave			3.51
east amphibole dike	60	2.99	f	2.099	15.0	3.55
			s	2.018	12.5	4.10
			t	2.056	14.3	3.65
			ave			3.77
west amphibole dike	61	3.09	f	2.052	15.5	3.36
			s	2.014	14.0	3.65
			t	2.037	14.0	3.70
			ave			3.57
west amphibole dike	63	3.07	f	1.976	14.3	3.51
			s	1.997	14.0	3.62
			t	1.826	12.0	3.87
			ave			3.67
biotite schist	65	2.71	f	2.002	19.0	2.68
			s	1.932	17.0	2.89
			t	2.005	15.8	3.22
			ave			2.93
Cutler aplite	66	2.66	f	1.998	17.0	2.98
			s	1.957	15.5	3.21
			t	1.998	15.0	3.38
			ave			3.19
Cutler aplite	67	2.66	f	2.021	14.5	3.54
			s	2.024	17.0	3.02
			t	2.018	17.6	2.91
			ave			3.16
Ordovician limestone	69	2.76	f	2.105	16.0	3.34
			s	2.030	16.7	3.09
			t	2.063	16.0	3.27
			ave			3.23
vein quartz	70	2.64	f	1.673	11.5	3.70
			s	1.817	11.3	4.08
			t	1.962	11.8	4.22
			ave			4.00

Lithology	Cube No.	Density g/cc	Face*	Dimen. Inch	Time μsec	V_s km/sec
Littleton granite gneiss	71	2.72	f	1.952	17.5	2.83
			s	1.931	17.5	2.80
			t	1.891	18	2.67
			ave			2.76
Quincy granite	75	2.65	f	2.026	21.0	2.45
			s	2.027	20.5	2.51
			t	1.983	21.5	2.34
			ave			2.44

* f = front
s = side
t = top

TABLE 5.--Elastic constants and related principal facts.

Lithology	Cube No.	density g/cc	ave V_P km/sec	ave V_S km/sec	λ 10^{10} dynes/cm^2	μ 10^{10} dynes/cm^2	σ	K 10^{10} dynes/cm^2	E 10^{10} dynes/cm^2	$\frac{V_S}{V_P}$
Neg. iron	2	3.05	5.40	3.37	19.6	34.6	0.18	42.7	81.8	0.62
bio. am. sch.	5	2.95	5.32	3.28	20.0	31.7	0.19	41.2	75.7	0.61
serpentin.	9	2.87	5.54	3.52	17.0	35.6	0.16	40.7	82.6	0.64
Mesn. qtz.	19	2.67	5.85	3.46	27.4	32.0	0.23	48.8	78.7	0.59
Esp. arg.	42	2.87	5.27	2.78	35.3	22.2	0.31	50.1	58.0	0.55
Serp. qtz.	43	2.62	4.88	3.02	14.6	23.9	0.19	30.5	56.9	0.62
Serp. qtz.	44	2.63	5.13	3.22	14.7	27.3	0.18	32.9	64.1	0.63
Sud. gab	56	2.99	6.50	3.02	71.8	27.3	0.36	90.0	74.3	0.56
oliv. diab	57	3.10	6.20	3.73	32.9	43.1	0.22	61.7	104.9	0.60
oliv. diab	58	3.02	6.26	3.48	45.2	36.6	0.28	69.6	93.3	0.56
oliv. diab	59	3.01	6.19	3.51	41.2	37.1	0.26	65.9	93.7	0.57
e. amp. dike	60	2.99	6.65	3.77	47.2	42.5	0.26	75.6	107.3	0.57
w. amp. dike	61	3.09	6.74	3.57	61.6	39.4	0.30	87.9	102.8	0.53
w. amp. dike	63	3.07	6.79	3.67	58.8	41.3	0.29	86.4	107.0	0.56
biot. sch.	65	2.71	5.24	2.93	27.9	23.3	0.27	43.4	59.2	0.56
Cutl. apl.	66	2.66	4.81	3.19	7.40	27.1	0.11	25.4	60.0	0.66
Cutl. apl	67	2.66	4.67	3.16	4.88	26.6	0.08	22.6	57.2	0.67
Ordo. lm.	69	2.76	5.63	3.23	29.9	28.8	0.26	49.1	72.3	0.58
vein qtz.	70	2.64	6.22	4.00	17.7	42.2	0.15	45.8	96.9	0.64
Lit. gnis.	71	2.72	4.47	2.76	12.9	20.7	0.19	26.7	49.4	0.62
Quin. gran.	75	2.65	4.20	2.44	15.2	15.8	0.24	25.7	39.3	0.57

FIGURE 1

Cube number	Lithology
10, 11	granite gneiss
66, 67	Cutler aplite
72, 73	Grenville granite gneiss

Figure 1.--Great Lakes Region Showing Principal Collection Areas.

FIGURE 2

Cube number	Lithology
1, 2, 3	Negaunee iron formation-Republic
4, 5, 76	biotite amphibolite schist
6, 7	Mona schist-Lighthouse Point
8, 9	serpentinite
12, 13	Negaunee iron formation-Ishpeming
14, 15	Siamo slate
16, 17	Mona schist-Chocolay
18, 19	Mesnard quartzite
20, 21	Kona dolomite
22	basalt
23	quartz latite porphyry
24, 25	amphibole biotite schist
26, 27	Republic granite

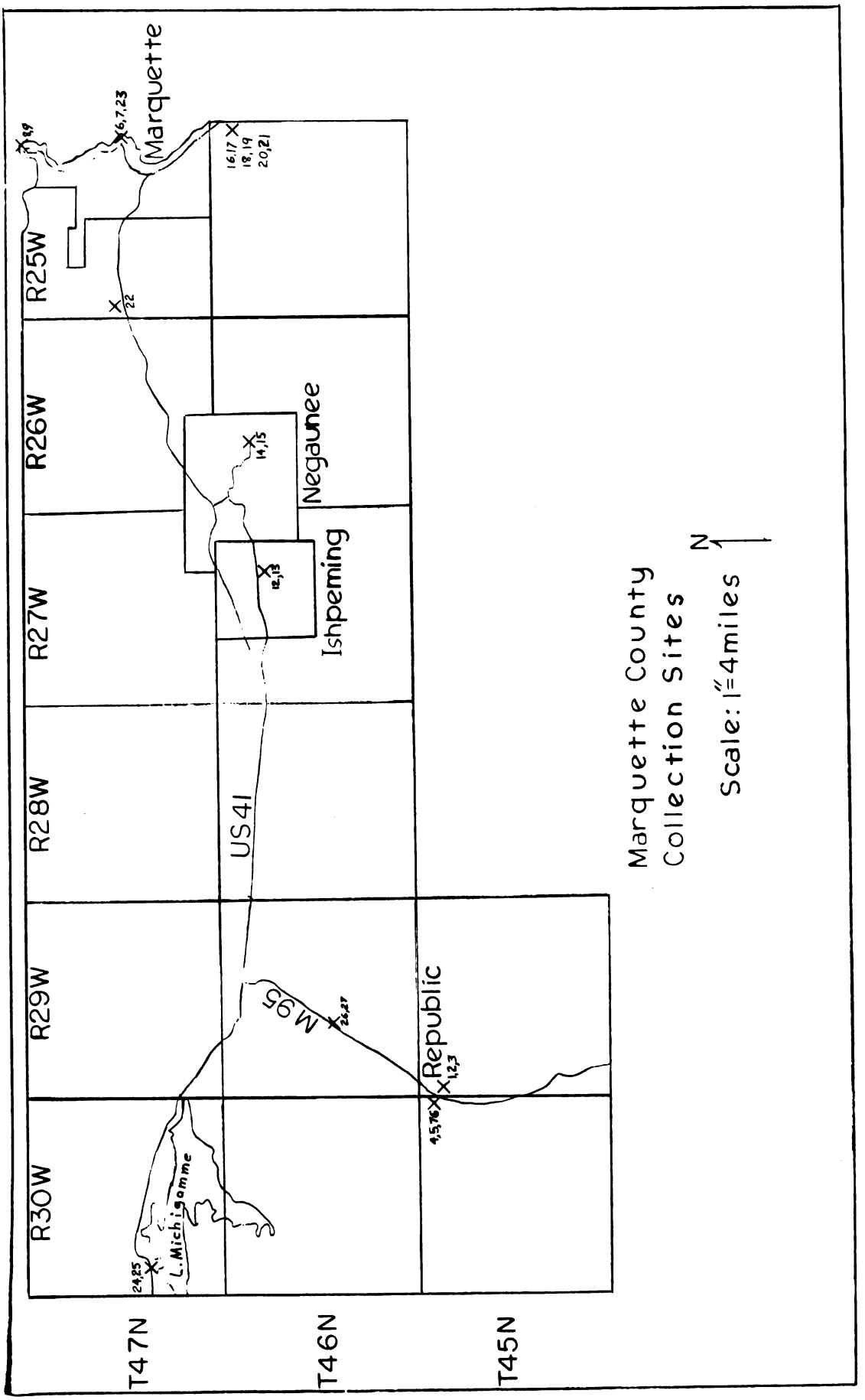

Figure 2.--Marquette County Collection Sites.

FIGURE 3

Cube number	Lithology
31, 32	McKim graywacke
33, 34	Mississagi quartzite
35, 36	Espanola limestone-Haystack Harbor
37, 38	Espanola limestone-island TP2203
39, 40	Espanola argillite-Clear Lake
41, 42	Espanola argillite-Pot Hole Portage
43, 44	Serpent quartzite
45, 46, 47	Gowganda argillite-Raven Lake
48, 49	Gowganda argillite-Whitefish Falls
50	Gray Lorrain quartzite
51	Pink Lorrain quartzite
52	White Lorrain quartzite
53, 54	Banded Lorrain quartzite
55, 56	Sudbury gabbro
57, 58, 59	Olivine diabase
60	East amphibole dike
61, 62, 63	West amphibole dike
64, 65	Biotite schist
68, 69	Ordovician limestone
70	Vein quartz

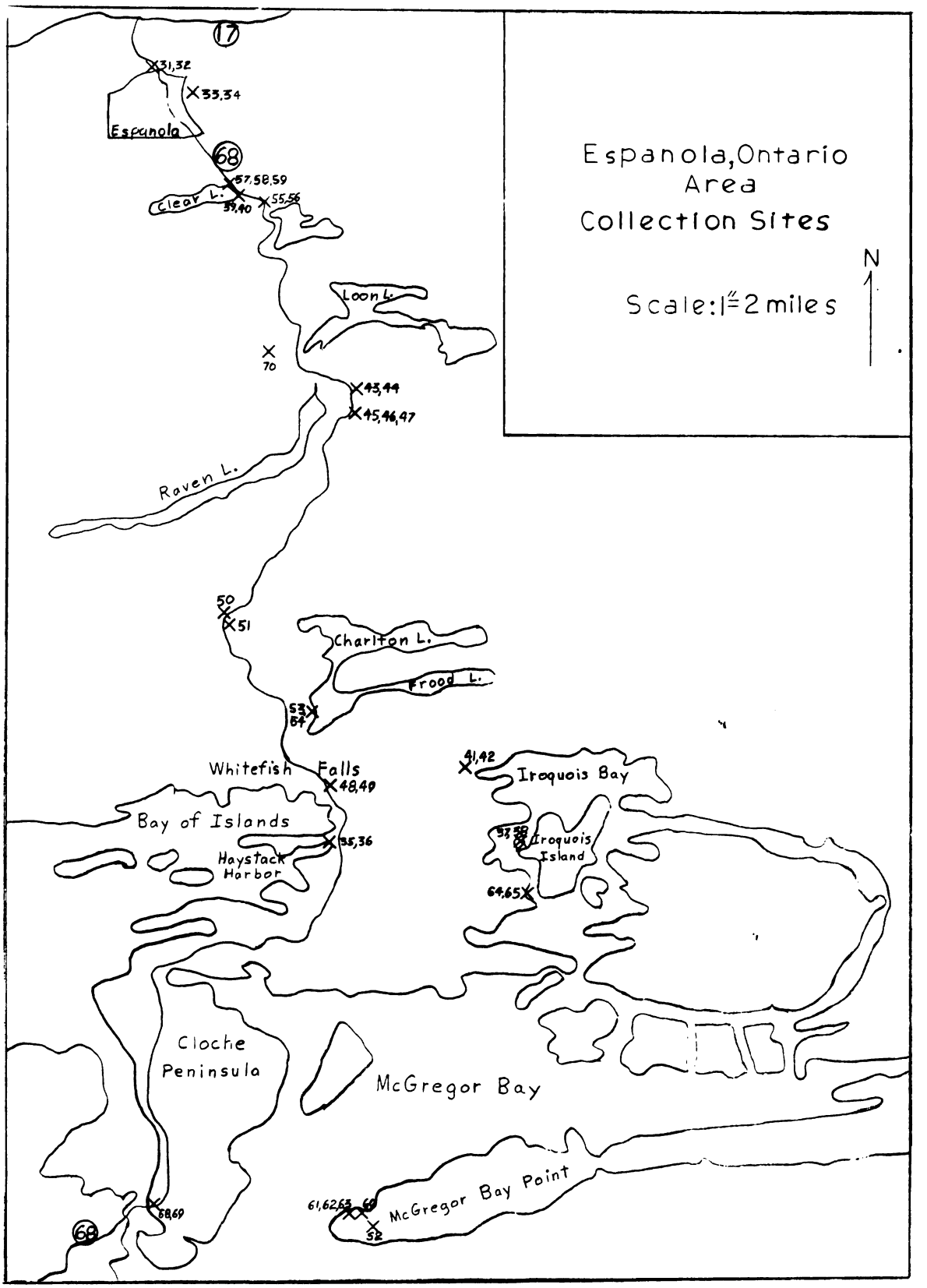

Figure 3.--Espanola, Ontario Area Collection Sites.

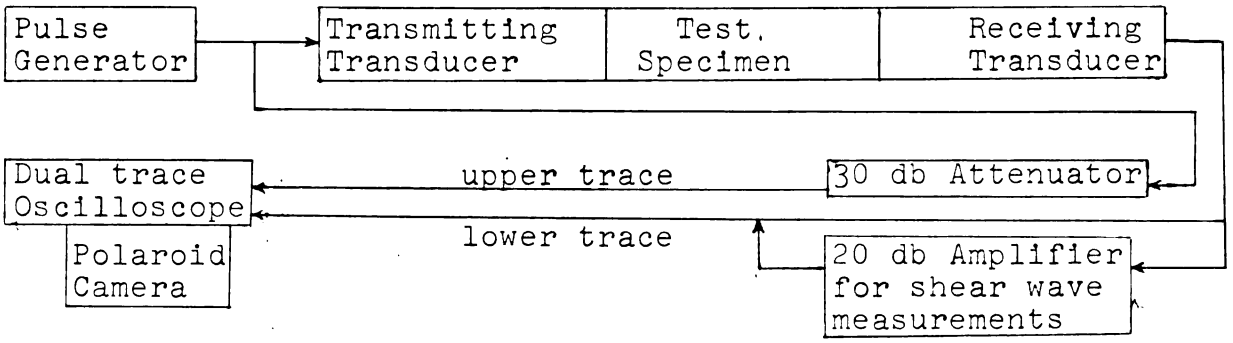

Equipment List

1. Pulse Generator, Hewlett-Packard Model 212A
2. Oscilloscope, Tektronix Type 545A
3. Amplifier, Hewlett-Packard Model 450A
4. Polaroid Camera
5. Transducers
6. Attenuator, 30 db, Empire Devices

Figure 4.--Block diagram of instrumental set-up for ultrasonic pulse measurements.

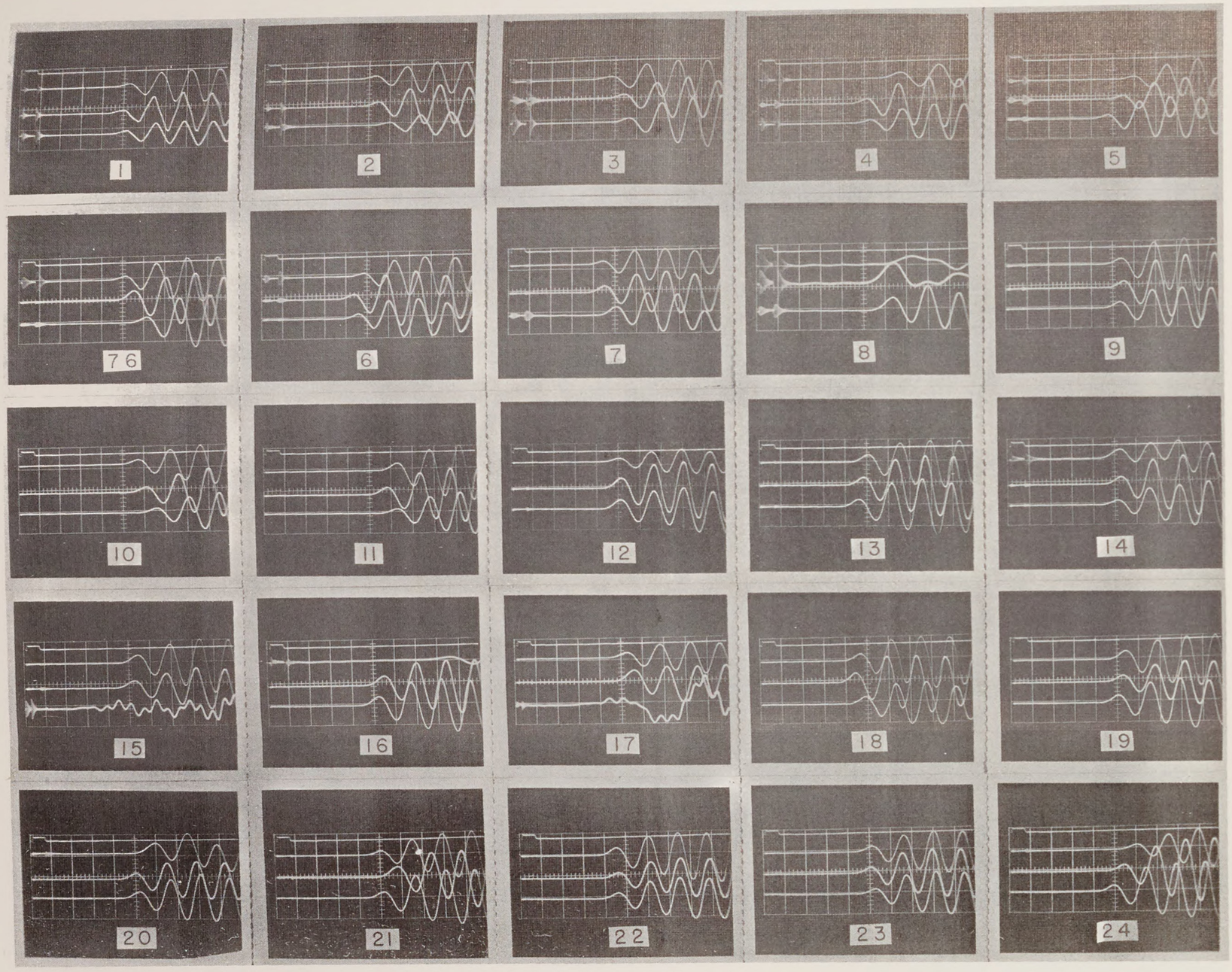

Figure 5.--Compressional Wave Photographs of Cubes 1 to 24, including cube 76.

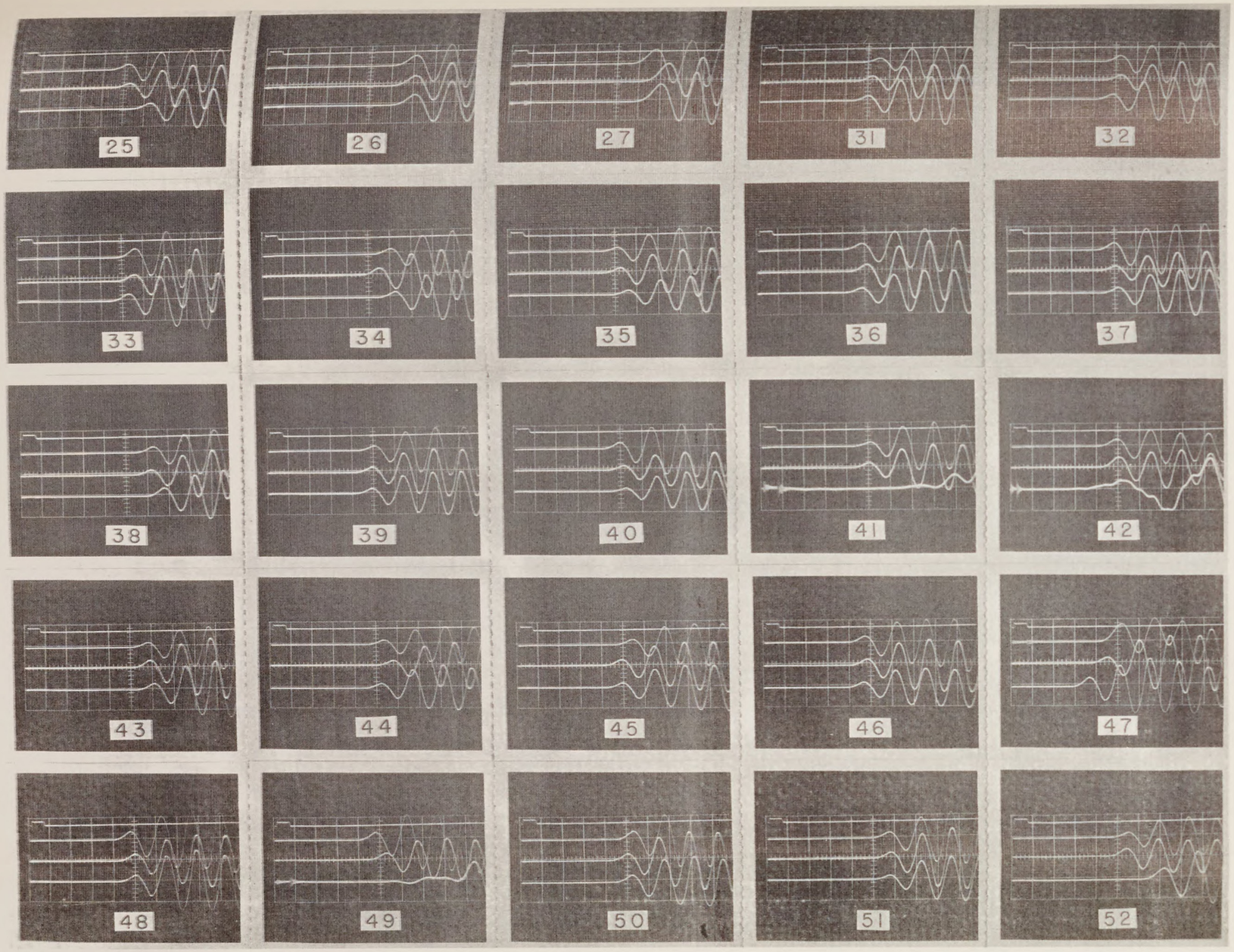

Figure 6.--Compressional Wave Photographs of Cubes 25 to 52.

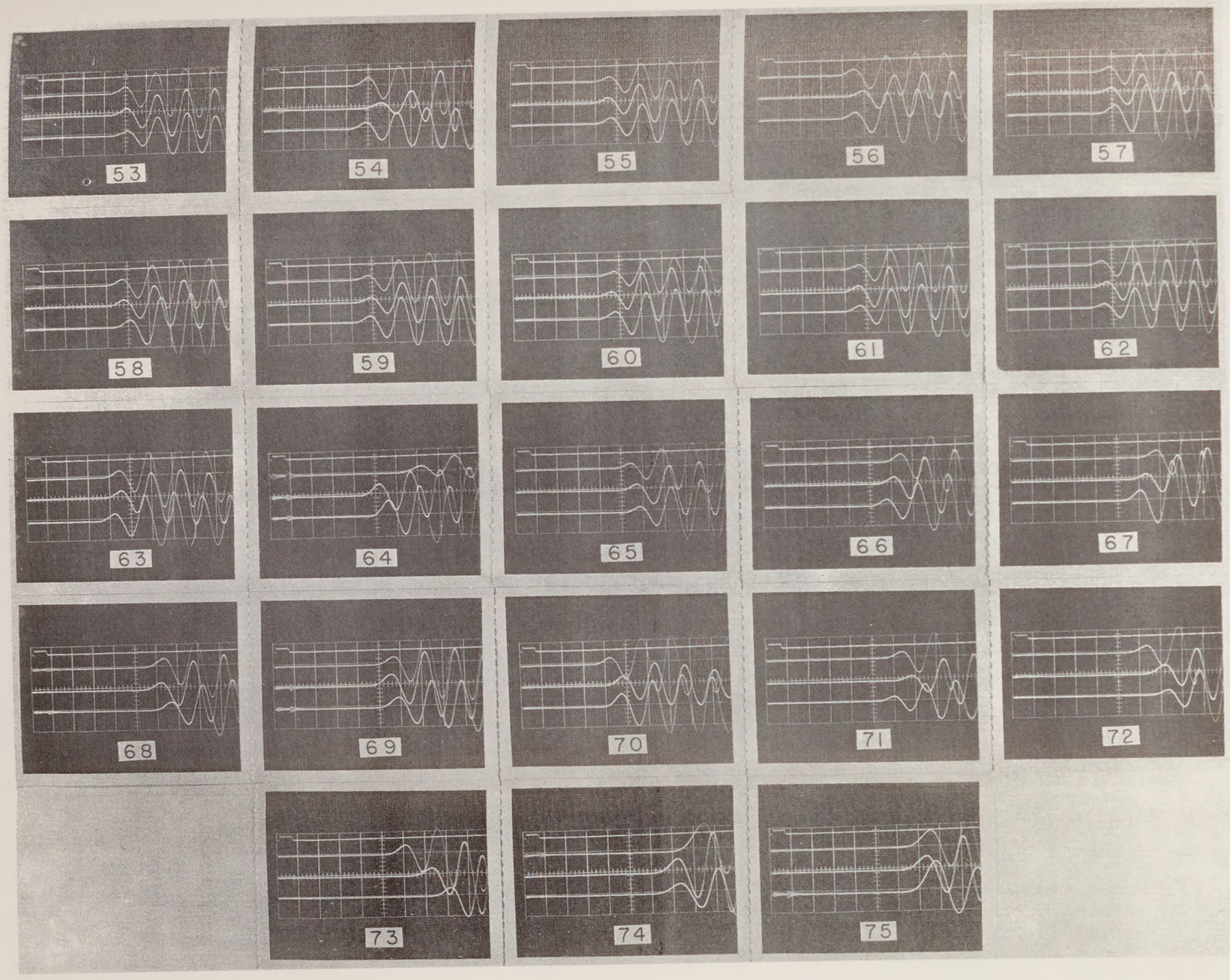

Figure 7.--Compressional Wave Photographs of Cubes 53 to 75.

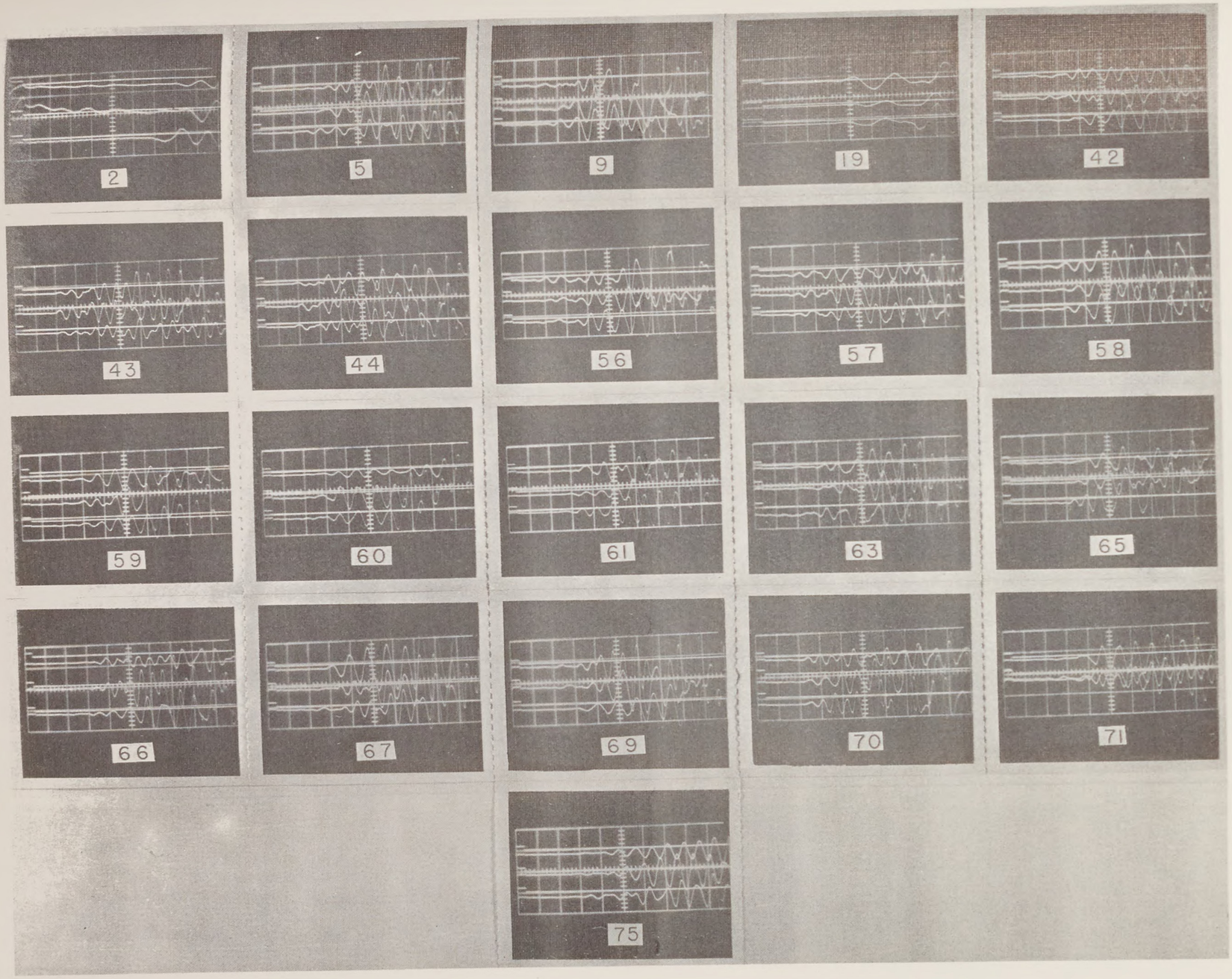

Figure 8.--Shear Wave Photographs of 21 Cubes.

FIGURE 9

Photograph	Description	Sweep speed (μsec/cm)
a	Brass V_p	2, 5, 10
b	Brass V_s	10, 20, 50
c	Magnesium V_p	0.5, 0.5, 2, 10
d	Magnesium V_s	2, 2, 5, 10
e	Woeber specimen 2, V_p	2
f	Woeber specimen 11, V_p	1
g	Woeber specimen 33, V_p	2, 5, 2
h	Woeber specimen 37, V_p	1
i	Woeber specimen 43, V_p	2, 1, 2
j	Woeber specimen 11, V_s	2, 5, 5
k	Woeber specimen 33, V_s	5
l	Woeber specimen 37, V_s	5, 2, 2,
m	Woeber specimen 43, V_s	2, 5, 5
n	Cube 1, front, reproducibility	2
o	Repeated V_p, cube 3, front	1
	cube 7, side	2
	cube 8, front	2
	cube 8, side	2
p	Repeated V_p, cube 15, top	5
	cube 16, front	2
	cube 17, top	2
	cube 30, front	2
q	Repeated V_p, cube 41, top	2
	cube 42, side	2
	cube 42, top	2
	cube 49, top	2
	cube 54, side	2

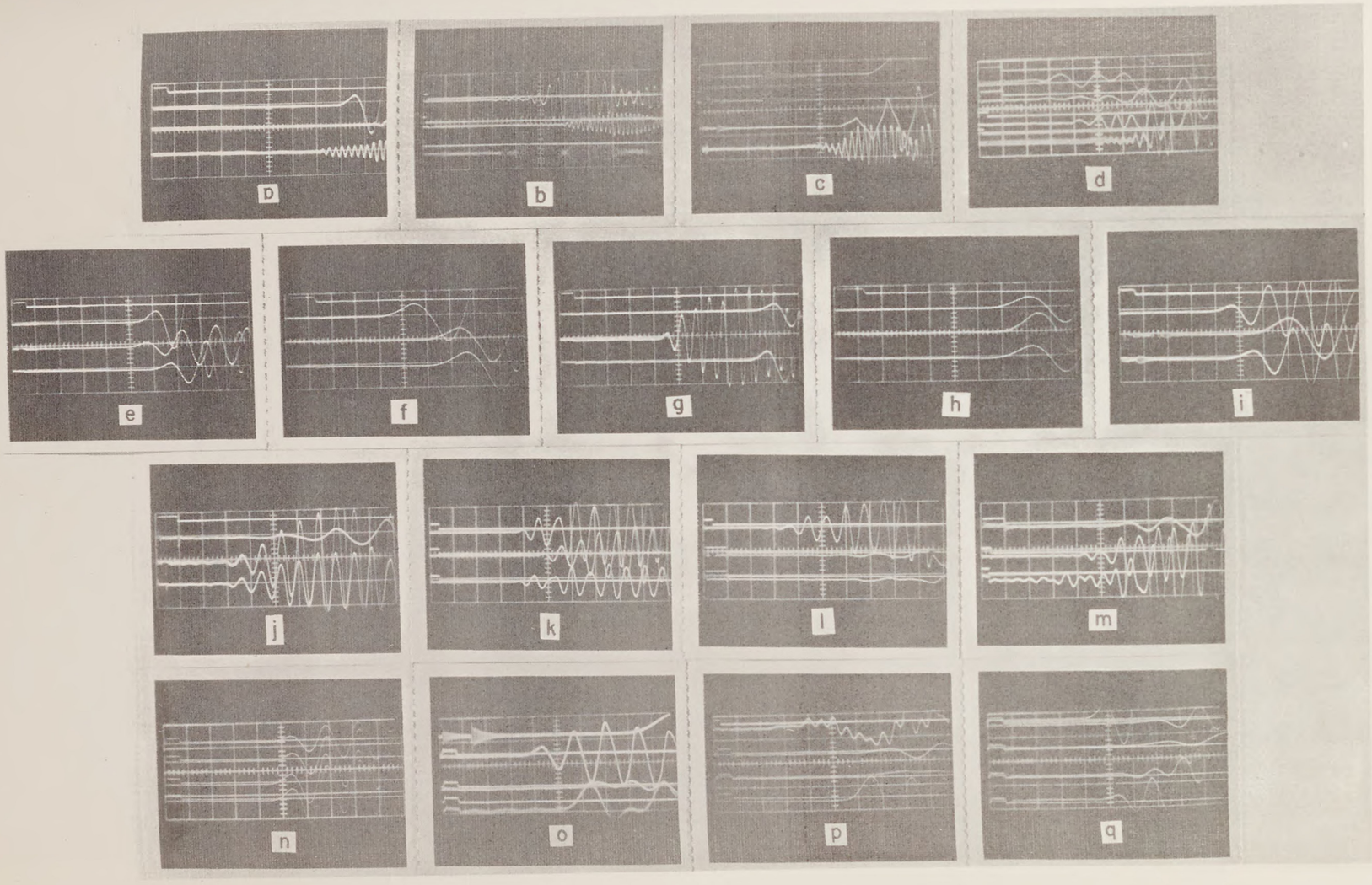

Figure 9.--Compressional and Shear Wave Photographs on Standards.

Ph

a

b

c

d

e

f

g

h

i

j

k

l

m

n

o

p

q

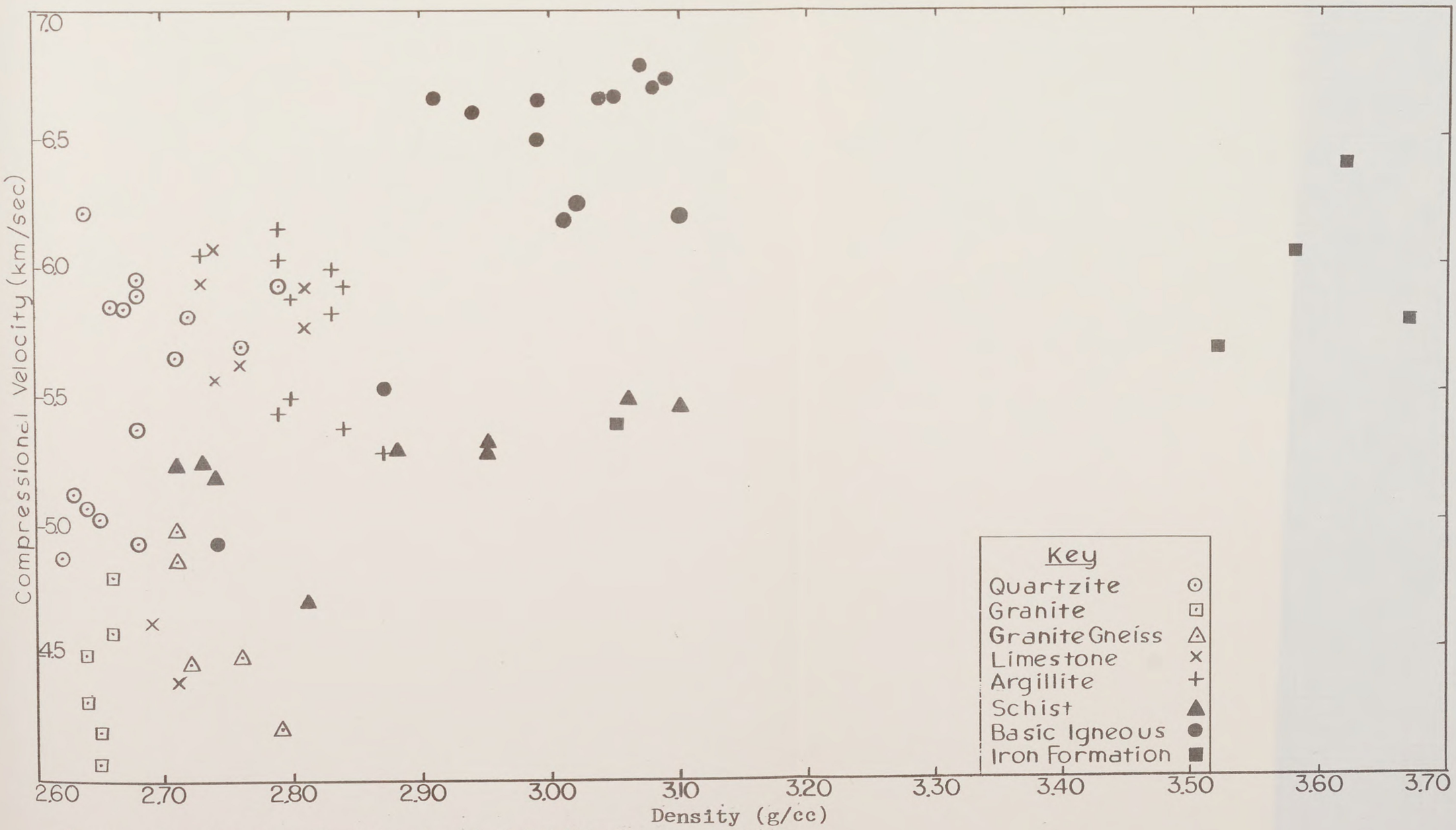

Figure 10.--Average Compressional Velocity Versus Density.

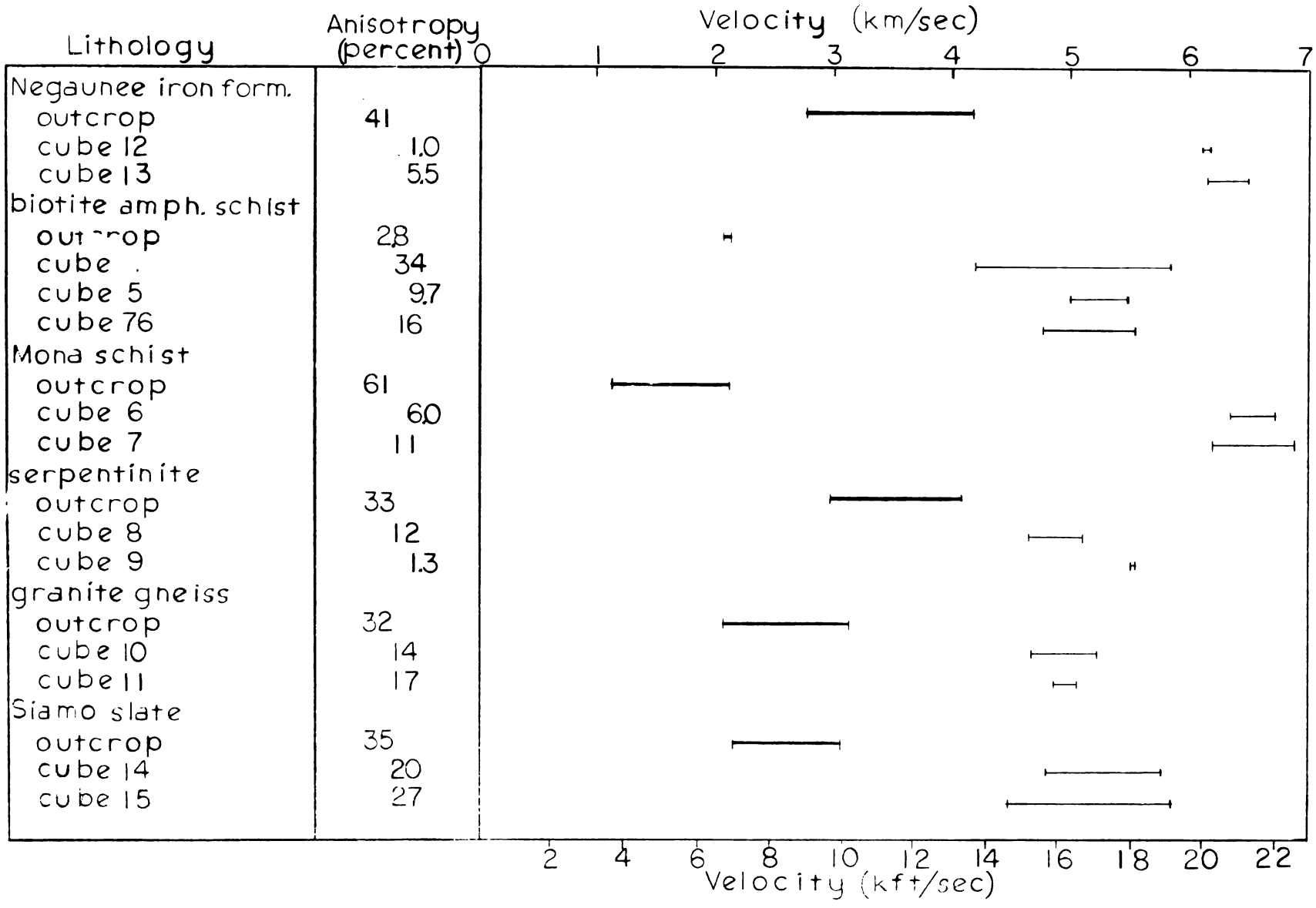

Figure 11.--Comparison of Laboratory and Field Determined Compressional Velocities and Anisotropies.

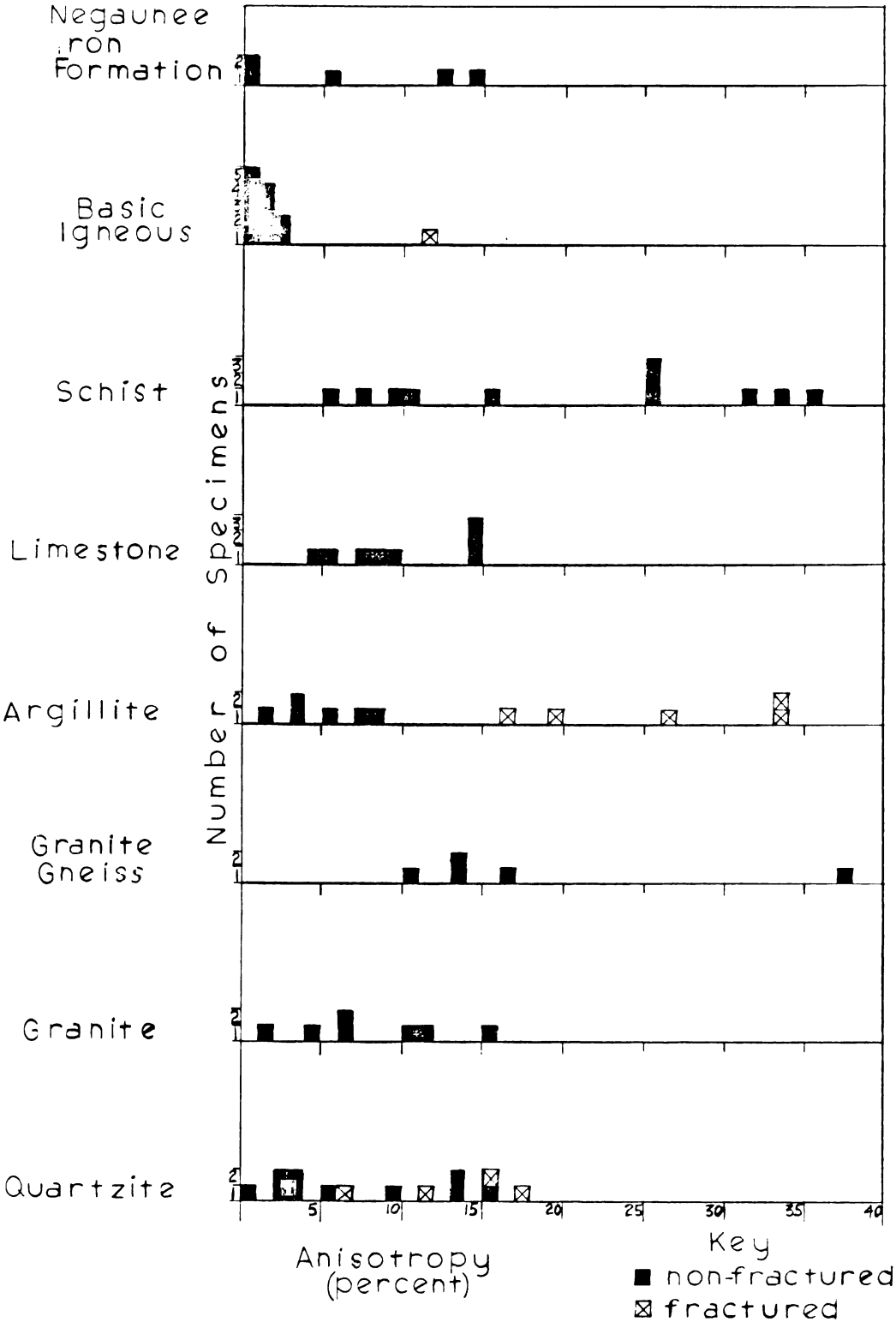

Figure 12.--Distribution of Velocity Anisotropy Among Lithologic Groups.

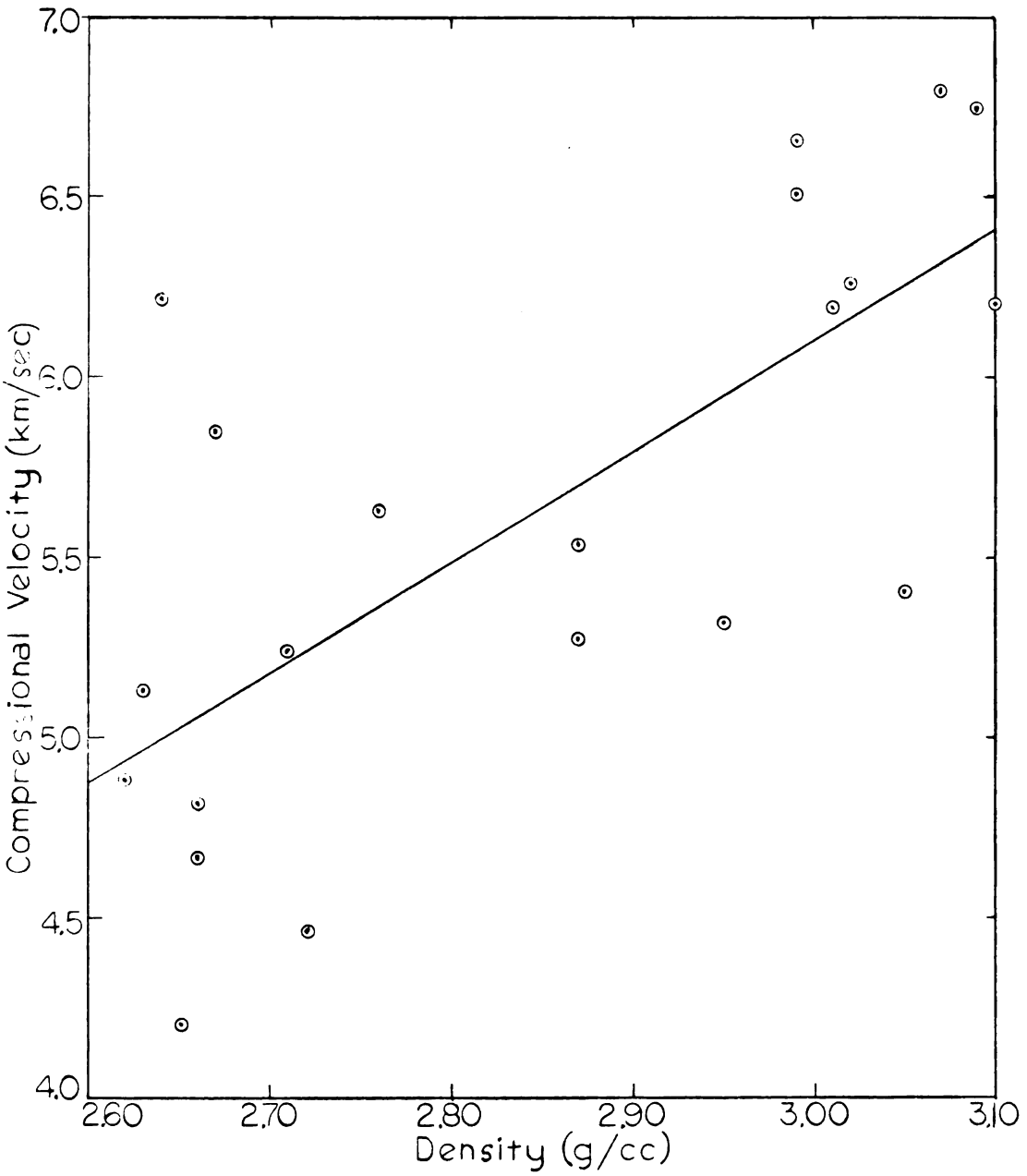

Figure 13.--Average Compressional Velocity Versus Density for 21 Specimens.

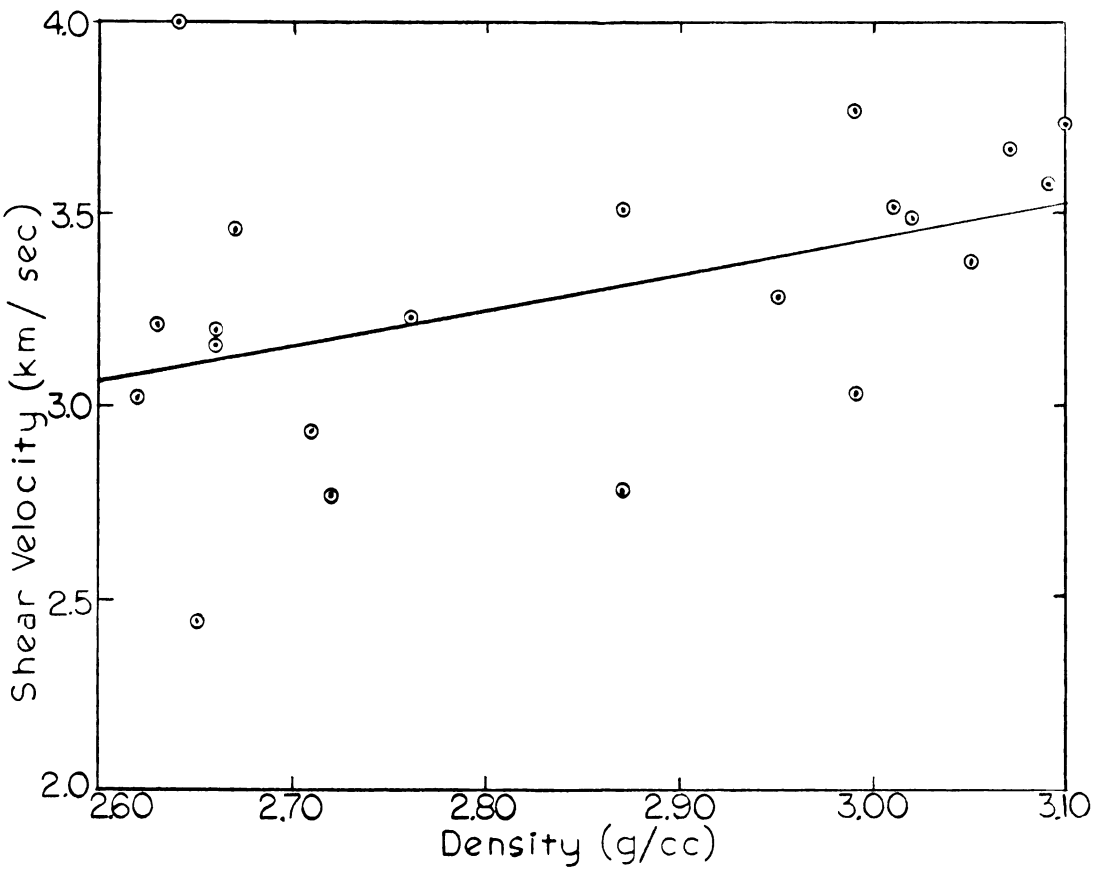

Figure 14.--Average Shear Velocity Versus Density.

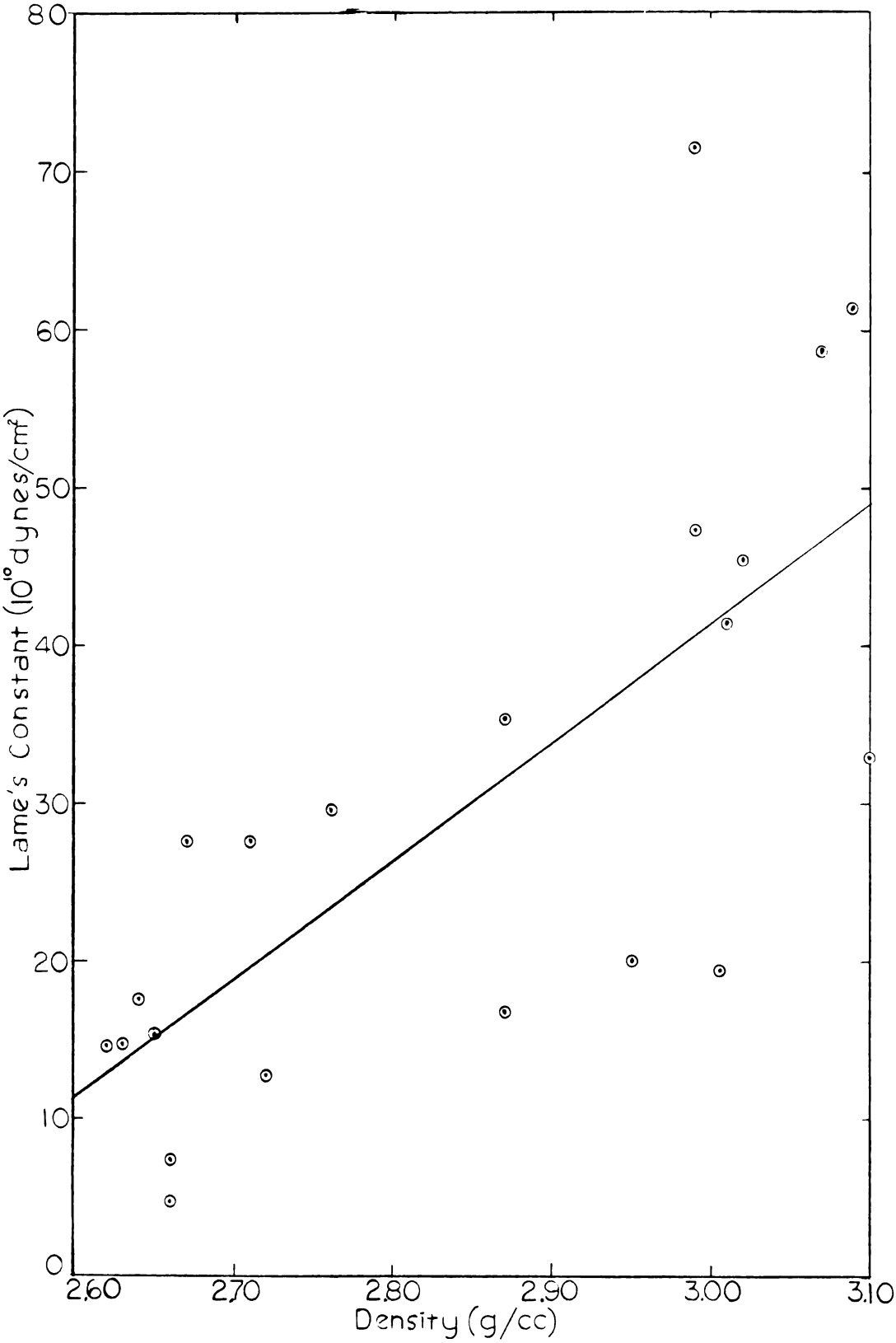

Figure 15.--Lame's Constant Versus Density.

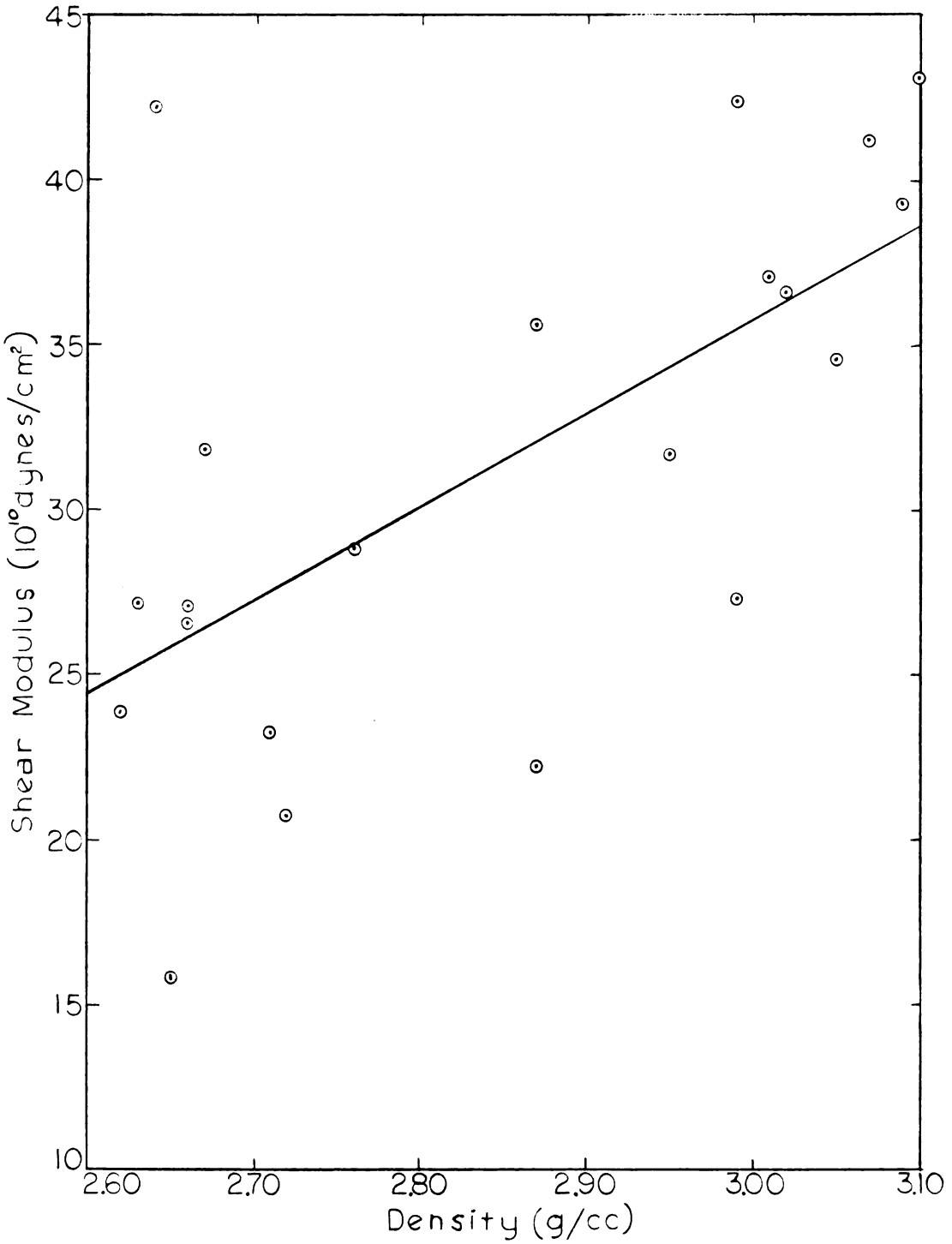

Figure 16.--Shear Modulus Versus Density.

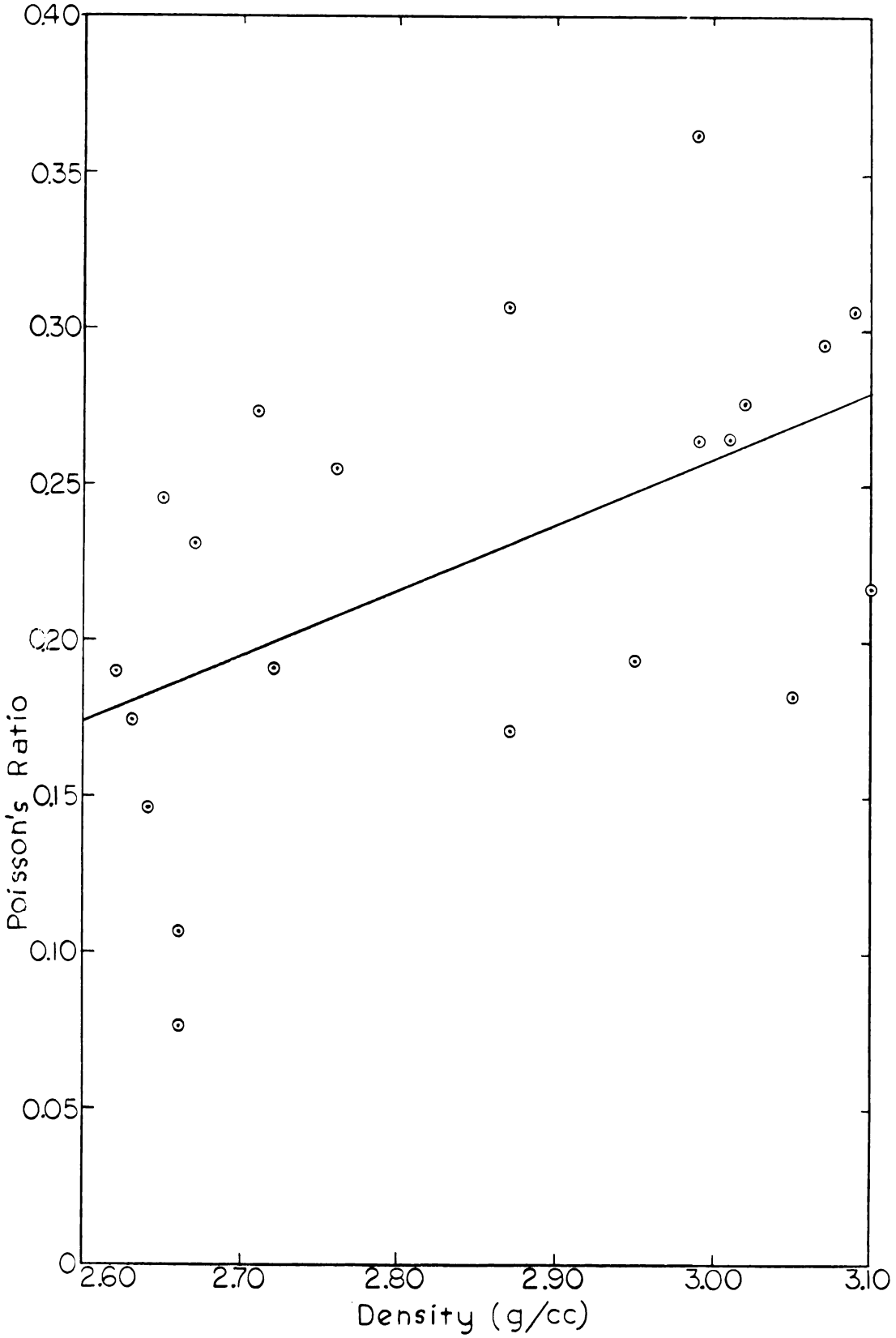

Figure 17.--Poisson's Ratio Versus Density.

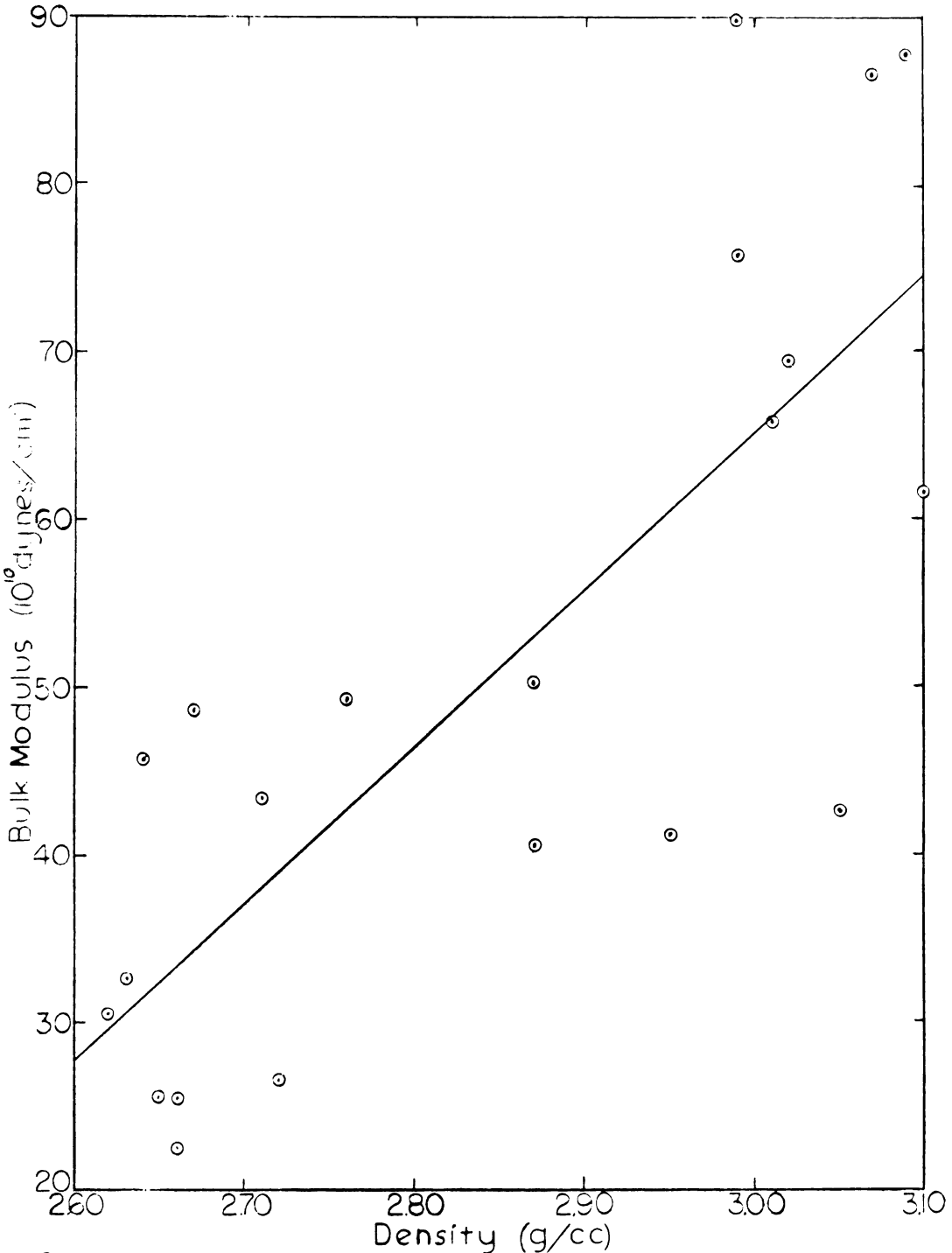

Figure 18.--Bulk Modulus Versus Density.

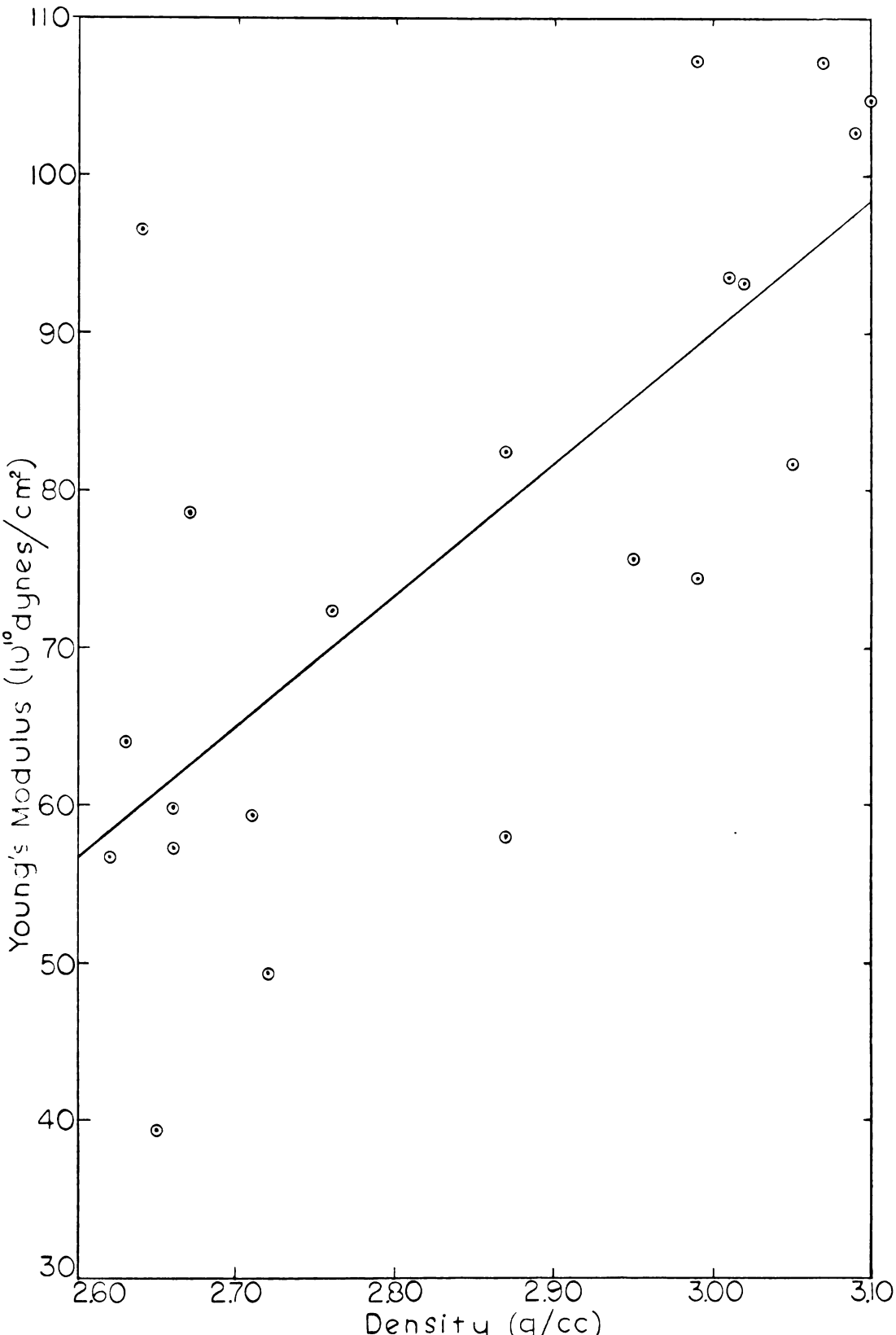

Figure 19.--Young's Modulus Versus Density.